

Neural Signals Generate Clinical Notes in the Wild

Jathurshan Pradeepkumar¹ Zheng Chen² Jimeng Sun¹

Abstract

Generating clinical reports that summarize abnormal patterns, diagnostic findings, and clinical interpretations from long-term EEG recordings remains labor-intensive. We curate a large-scale clinical EEG dataset with 9,922 reports paired with approximately 11,000 hours of EEG recordings from 9,048 patients. We therefore develop CELM, the first clinical EEG-to-Language foundation model capable of summarizing long-duration, variable-length EEG recordings and performing end-to-end clinical report generation at multiple scales, including recording description, background activity, epileptiform abnormalities, events/seizures, and impressions. Experimental results show that, with patient history supervision, our method achieves 70%–95% average relative improvements in standard generation metrics (e.g., ROUGE-1 and METEOR) from 0.2–0.3 to 0.4–0.6. In the zero-shot setting without patient history, CELM attains generation scores in the range of 0.43–0.52, compared to baselines of 0.17–0.26. CELM integrates pretrained EEG foundation models with language models to enable scalable multimodal learning. We release our model and benchmark construction pipeline at

1. Introduction

Electroencephalography (EEG) records long-term, real-time neuronal activity with millisecond-level temporal resolution and is widely used in hospitals for neurological diagnosis, such as epilepsy (Kotoge et al., 2025) and sleep health (Yang et al., 2023). However, writing clinical reports to summarize diagnostic findings over long-term EEG recordings remains a labor-intensive process. Typically, neurologists visually inspect EEG signals to assess brain activity and then compose clinical reports that document abnormal patterns (i.e., EEG

phenotypes) and their clinical interpretations (Tatum IV et al., 2016). Moreover, this task requires substantial domain knowledge and extensive clinical experience, which in turn incur long-term training costs and require continual updates as new EEG phenotypes or waveforms are identified (Biswal et al., 2019).

To support this profound clinical practice, several automated clinical EEG report generation models based on advanced deep learning techniques have been proposed (Biswal et al., 2019; Lee et al., 2023; Yin & Shin, 2025). These methods aim to encode EEG recordings into latent representations that capture temporal structure and clinically relevant phenotypes, which are then decoded into clinical reports. However, existing methods remain limited in several aspects. ① Conceptually, some works formulate report generation as a phenotype classification or retrieval problem followed by text decoding. They do not model EEG-to-report generation as an end-to-end learning task, and the misalignment between classification and generation objectives does not guarantee optimal report generation. ② Methodologically, these methods operate on short EEG segments and fixed-context templates. They fail to model long-term temporal context and global diagnostic reasoning required for interpreting long-duration EEG data. Moreover, fixed-context templates prevent multi-granularity report generation beyond predefined categories. ③ Practically, these methods are developed as task-specific models, each tailored to a narrow reporting objective (e.g., impression-only reports) (Lee et al., 2023). In contrast, clinical practice requires multi-level reporting, where neurologists routinely construct overall EEG summaries and section-wise outputs, including impressions, interpretations, and event or seizure annotations.

Present work. We introduce CELM, which, to the best of our knowledge, is the first clinical EEG-to-language foundation model (ELM) capable of generating EEG reports at multiple scales. We train and evaluate CELM on 9,922 clinical reports paired with approximately 11,000 hours of EEG recordings from 9,048 patients, spanning both clinical context-conditioned and zero-context settings, and covering key report sections including EEG description, background activity, epileptiform abnormalities, events/seizures, and impressions/interpretations.

Our motivation stems from recent advances in multimodal

¹Siebel School of Computing and Data Science, University of Illinois Urbana-Champaign, IL, USA. ²SANKEN, Osaka University, Japan. Correspondence to: Jathurshan Pradeepkumar <jp65@illinois.edu>, Zheng Chen <chenz@sanken.osaka-u.ac.jp>, Jimeng Sun <jimeng@illinois.edu>.

foundation models that enable text generation from non-text modalities (e.g., images and speech) (Bordes et al., 2024; Shen et al., 2025). Recent studies have begun to incorporate EEG signals into language-based modeling frameworks (Ndir et al., 2025; Gijsen & Ritter, 2025). However, they primarily leverage text supervision to enhance EEG classification and do not support EEG-to-text report generation.

To tackle aforementioned limitations, the contributions of this paper lie in: ❶ Conceptually, we formulate neurological clinical report generation as an *EEG-to-Language foundation modeling* problem. CELM enables end-to-end training and generation by directly translating raw EEG recordings into clinical text, without relying on intermediate phenotype classification or template-based pipelines. ❷ Methodologically, we introduce the first EEG-to-language multimodal framework, comprising three core components: (i) epoch-aggregated tokenization that produces compact representations from variable-length recordings, (ii) sequence-aware alignment that captures inter-epoch temporal dependencies, and (iii) prompt fusion for conditional report generation. Importantly, our model design harnesses the representation capabilities of pretrained EEG foundation models and LLMs while enabling flexible generation across multiple clinical settings. ❸ Practically, we introduce the first ELM benchmark construction pipeline based on the Harvard Electroencephalography Database (Sun et al., 2025; Zafar et al., 2025), which contains approximately 12k clinical reports paired with about 100k hours of EEG recordings from 10k patients. Rather than requiring access to the raw, unstructured 200TB corpus and associated metadata, our pipeline enables efficient filtering of EEG recordings matched to reports. We release all source code to support further evaluation and development.

Experimental results show that CELM consistently outperforms all baselines across all settings. With patient history, it achieves 70%–95% average relative improvements, with standard generation metrics (e.g., METEOR (Banerjee & Lavie, 2005) and ROUGE-1 (Lin, 2004)) from 0.2–0.3 to 0.4–0.6 across diverse cases. In the zero-context setting without patient history, CELM achieves generation scores in the range of 0.43–0.52, compared to baselines of 0.17–0.26. We provide multi-perspective case analyses to shed light on future ELM development.

2. Related Work

EEG-to-Language Modeling. Existing work at the intersection of EEG and natural language can be broadly categorized into two paradigms: (1) EEG-to-language decoding and (2) text-enhanced EEG representation learning. The goal of EEG-to-language decoding is to reconstruct textual content from concurrent EEG recordings of subjects reading or imagining speech (Herff et al., 2015; Wang & Ji,

2022). This line of work spans both invasive approaches using electrocorticography (ECoG) (Makin et al., 2020; Willett et al., 2023) and non-invasive methods based on scalp EEG (Wang & Ji, 2022; Duan et al., 2023; Zhou et al., 2024). However, these methods assume precise EEG–text alignment, whereas clinical EEG consists of heterogeneous events embedded in long, continuous recordings spanning hours to days (Sun et al., 2025; Zafar et al., 2025). The second paradigm leverages clinical notes as auxiliary supervision to enhance EEG representation learning, rather than decoding language directly from neural activity. Inspired by vision–language pretraining frameworks (Radford et al., 2021), a recent work (Ndir et al., 2025) aligns EEG data with clinical report text in a shared feature space. However, it remains focused on discriminative objectives and does not support automated clinical report generation.

Clinical EEG Report Generation. An early attempt at EEG report generation, EEGtoText (Biswal et al., 2019), proposed a two-stage pipeline that first classifies EEG phenotypes, and then generates report text via a text decoder conditioned on the classified labels. However, this relies on intermediate phenotyping as a bottleneck, limiting the capabilities to capture nuanced clinical findings beyond pre-defined categories. While some attempts jointly learn EEG encoders and text decoders (Lee et al., 2023), they rely on fixed segmentation and template-based generation (Yin & Shin, 2025). As a result, these methods fall short of end-to-end clinical report generation from long-duration EEG recordings. We address the above challenges by introducing the first family of EEG–Language foundation models.

EEG Foundation Models. Recent years have witnessed rapid advances in EEG foundation models. BENDR (Kostas et al., 2021), BIOT (Yang et al., 2023), LaBraM (Jiang et al., 2024), TFM-Tokenizer (Pradeepkumar et al., 2025), EEGPT (Wang et al., 2024a), LUNA (Döner et al., 2025), REVE (Ouahidi et al., 2025), and CBraMod (Wang et al., 2024b) introduce increasingly scalable tokenization and representation learning frameworks that achieve strong transfer on diverse EEG tasks. These models are predominantly encoder-only and are optimized for classification tasks, leaving generative objectives largely unexplored. Our CELM is designed for clinical EEG report generation, and notably, it is fully compatible with existing foundation models, which can be directly leveraged as EEG encoders.

3. EEG-Report Benchmark Construction

Currently, no publicly available benchmark provides structured EEG–report pairs for training and evaluating EEG-to-Language Models (ELMs). In this work, we leverage two resources from the *Brain Data Science Platform*: (1) the Harvard Electroencephalography Database v4.1 (Zafar et al., 2025; Sun et al., 2025), which contains approximately 10k

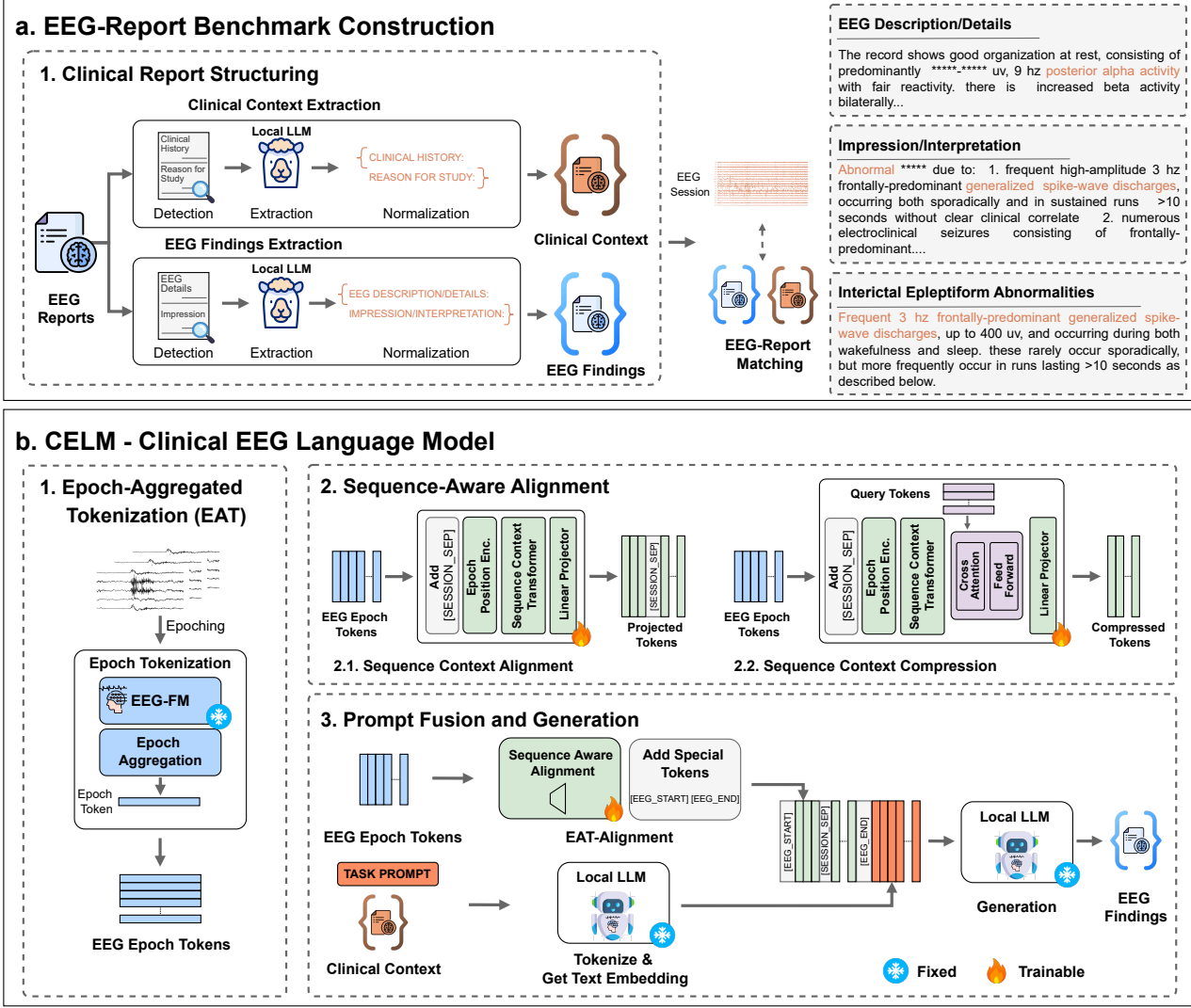


Figure 1. Overview of our framework. (a) EEG–Report benchmark construction pipeline, including clinical report structuring (Section 3.1), matching reports to EEG sessions, and examples of standardized report sections. (b) The proposed Clinical EEG Language Model (CELM) comprises (b.1) Epoch-Aggregated Tokenization, (b.2) Sequence-Aware Alignment, and (b.3) Prompt Fusion and Generation.

clinical reports paired with about 100k hours of EEG recordings from 10,886 patients across multiple hospital sites, and (2) the Electronic Health Records (EHR) Repository with corresponding unstructured neurology reports. The EHR repository links reports to one or more EEG sessions via temporal alignment between EDF start times and report timestamps. Therefore, we construct an EEG–report benchmark using a dedicated processing pipeline (Figure 1a). Specifically, Section 3.1 describes how neurology reports are extracted and organized based on whether their content is inferable from EEG data. Section 3.2 details the preprocessing and standardization of the matched EEG recordings.

3.1. Clinical Report Structuring

Neurology reports can be broadly decomposed into two types of sections: (1) *Clinical Context*, which contains information such as patient history and monitoring indications

that cannot be inferred from EEG signals, and (2) *EEG Findings*, which describe EEG observations and clinical interpretations that are directly inferable from EEG recordings. This distinction is critical for evaluating clinical ELMs, as sections within EEG Findings provide the appropriate ground truth for benchmarking a model’s ability to generate clinical narratives from EEG signals.

A key challenge lies in reliably extracting and structuring these sections without information loss. Substantial variability in reporting styles and formatting makes manual extraction infeasible at scale. We therefore propose a three-stage automated pipeline to extract and structure reports.

➤ *Section Detection:* first, we curate a comprehensive list of candidate section headers under each category and detect their presence using string matching.

➤ *Section-wise Extraction:* second, for each detected sec-

tion, we employ a local LLM (Meta-Llama-3-8B-Instruct) to extract the corresponding text using simple copy-based prompts. This detect-then-segment strategy avoids hallucinations and cross-section contamination that arise when extracting multiple sections jointly. Local deployment is required, as data use agreements prohibit sending clinical reports to proprietary cloud-based LLMs.

➤ *Canonical Normalization*: finally, we standardize the extracted sections into canonical categories, including EEG description/details, impressions/interpretations, background activity, epileptiform abnormalities, and events/seizures.

3.2. EEG Preprocessing

Matched EEG recordings are preprocessed using a standard pipeline. Signals are first band-pass filtered between 0.1–75 Hz and notch filtered at 60 Hz to remove power-line interference. The recordings are then resampled to 200 Hz to ensure compatibility with existing EEG-only foundation models. Each recordings are segmented into non-overlapping 10-second windows, which is the typical temporal context used by current EEG foundation architectures. Finally, EEG channels are standardized to a 22-channel montage following the International 10-20 system. While the dataset contains reports matched to multiple EEG sessions, we filter to samples with single-session matches for training, validation, and evaluation. We then perform patient-level splitting into 60/20/20 training, validation, and test sets to ensure no patient overlap across splits, thereby preventing data leakage and producing a structured EEG–report benchmark.

4. CELM: Clinical EEG Language Model

This section introduces our CELM, consisting of three key components: *Epoch-Aggregated Tokenization*, *Sequence-Aware Alignment*, and *Prompt Fusion and Generation*. Unlike classification-oriented EEG models that learn discriminative representations for categorical labels, clinical ELMs must identify and aggregate clinically relevant information from EEG recordings to support report generation at multiple levels. To this end, Section 4.1 discusses the unique challenges of clinical ELMs and provides an overview of the model architecture and forward process. Sections 4.2, 4.3, and 4.4 then present the details of the three components.

4.1. Architecture and Forward Process

Clinical EEG introduces three unique challenges that prevent the direct adoption of existing multimodal paradigms, such as dictionary-based alignment or contrastive learning with fixed-length epochs (Ndir et al., 2025). Here, we design CELM with three corresponding steps:

➤ *Epoch-Aggregated Tokenization* addresses the extreme temporal scale of clinical EEG. EEG sessions span hours of high-frequency, multi-channel signals, resulting in at least

~ 31.7M+ data points per recording, far exceeding the context limits of modern LLMs (Grattafiori et al., 2024; Team et al., 2025; Yang et al., 2025).

➤ *Sequence-Aware Alignment* mitigates the loss of temporal context during alignment. EEG signals are inherently sequential, and naive projection into the LLM embedding space fails to preserve long-range temporal dependencies required for clinical interpretation.

➤ *Prompt Fusion and Generation* addresses weak EEG–text correspondence. Clinical reports aggregate findings over entire recordings without explicit temporal grounding, requiring the model to synthesize coherent clinical narratives from distributed EEG evidence.

Overall, given an input EEG recording, CELM processes the signal through above three stages. The recording is first transformed into compact epoch-level tokens via *Epoch-Aggregated Tokenization*, which reduces the extreme temporal scale. These tokens are then projected into the language model space through *Sequence-Aware Alignment*, enabling long-range temporal dependencies to be maintained across epochs. Finally, *Prompt Fusion and Generation* conditions the language model on the aligned EEG representations and optional clinical context to generate structured reports.

4.2. Epoch-Aggregated Tokenization

The fundamental bottleneck in developing ELMs is representing long EEG recordings within the LLM context constraints. A typical two-hour clinical EEG recording at 200 Hz across 22 channels yields $7,200 \times 200 \times 22 \approx 31.7M$ data points, far exceeding current LLM capacities, making raw sample-level tokenization infeasible. A common alternative is mini-window tokenization, leveraging pretrained EEG encoders that typically tokenize 1-second segments. However, naively applying this granularity to full recordings produces $\approx 158K$ tokens per session, still well beyond the context limits of most local LLMs (Grattafiori et al., 2024; Team et al., 2025; Yang et al., 2025). To overcome this limitation while harnessing pretrained EEG representations, we propose Epoch-Aggregated Tokenization (see Figure 1b.1).

Given an EEG recording session $\mathbf{X} \in \mathbb{R}^{N \times C \times T}$, where N , C , and T denote the number of epochs, channels, and time points per epoch (typically 10 seconds) respectively, we first tokenize mini 1s windows within each epoch using a pretrained EEG encoder. The resulting representations are then aggregated across mini-windows and channels to produce a single token per epoch, yielding a compact sequence of epoch tokens $\mathbf{E}_{\text{eeg}} \in \mathbb{R}^{N \times D_{\text{eeg}}}$, where D_{eeg} is the embedding dimension. The aggregation strategy is encoder-dependent. For example, CBraMod applies pooling (Wang et al., 2024b), whereas LaBraM (Jiang et al., 2024) and TFM-Tokenizer (Pradeepkumar et al., 2025) uses [CLS] pooling. This tokenization compresses the tokens by up to

$C \times T$ ($\sim 220 \times$ compared to mini-window tokenization), enabling EEG recordings to fit within LLM context limits.

4.3. Sequence-Aware Alignment

To enable EEG-conditioned clinical report generation and leverage LLMs' generative capabilities, EEG tokens must be aligned with the text embedding space of LLMs. In the vision-language setting, models such as LLaVA achieve this via a simple linear projection (Liu et al., 2023). However, this paradigm does not generalize well to EEG (Section 5.4) due to its inherent sequential nature, unlike static images. EEG signals exhibit long-range temporal dynamics across epochs that must be preserved during alignment. As a result, we face two key challenges: modeling long temporal dependencies and scalability for very long sequences. These challenges motivate the design of two alignment strategies in the proposed Sequence-Aware Alignment module (see Figure 1b.2): (1) Sequence Context Alignment, which preserves the full temporal sequence, and (2) Sequence Context Compression, which compresses the sequence into a fixed-length latent representation for memory-efficient alignment.

Sequence Context Alignment (SCA). Given a sequence of epoch tokens \mathbf{E}_{eeg} , we augment the sequence with learnable position encodings and [SESSION_SEP] tokens to differentiate EEG sessions. A lightweight linear-attention transformer (Wang et al., 2020; Katharopoulos et al., 2020) is then applied to capture the temporal structure across epochs. The resulting representations are subsequently projected through a linear layer into the language embedding space, yielding $\mathbf{H}_{\text{eeg}} \in \mathbb{R}^{N \times D_{\text{llm}}}$, where D_{llm} denotes the LLM embedding dimension.

Sequence Context Compression (SCC). In an attempt to tackle the memory constraints and improve scalability for long EEG sequences, we explore a compression strategy inspired by Perceiver architectures (Jaegle et al., 2021b;a). After encoding temporal structure among epoch tokens, a fixed set of learnable query tokens $\mathbf{Q} \in \mathbb{R}^{L \times D_{\text{eeg}}}$ ($L < N$) attend to the full sequence of epoch tokens via cross-attention. This compresses the variable-length EEG sequence into a fixed number of tokens, which are subsequently projected into the language embedding space, enabling efficient alignment for recordings of arbitrary duration.

4.4. Prompt Fusion and Generation

CELM generates clinical reports by conditioning a local LLM on EEG-derived representations jointly with clinical context when available (see Figure 1b.3). Given projected EEG tokens \mathbf{H}_{eeg} , we augment the sequence with special tokens [EEG_START] and [EEG_END] to distinguish EEG representations from text inputs. A task-specific prompt that specifies the target report sections, together with optional

clinical context (e.g., reason for study or clinical history), is tokenized using the LLM tokenizer to obtain text embeddings $\mathbf{H}_{\text{prompt}}$. The final input sequence to the LLM is formed by concatenation,

$$\mathbf{H}_{\text{in}} = [\text{[EEG_START]}; \mathbf{H}_{\text{eeg}}; \text{[EEG_END]}; \mathbf{H}_{\text{text}}] \quad (1)$$

which is processed autoregressively to generate a structured EEG report text. We employ instruction tuned Qwen3-4B (Yang et al., 2025) as our base LLM, CBraMod (Wang et al., 2024b) as our EEG encoder and perform supervised fine-tuning using the next-token prediction objective:

$$\mathcal{L} = - \sum_{t=1}^T \log P_{\theta}(y_t \mid H_{\text{input}}, y_{<t}) \quad (2)$$

During training, both the EEG encoder and LLM remain frozen, only the Sequence-Aware Alignment module is updated, enabling efficient adaptation while preserving pre-trained representations.

5. Experiments and Results

Datasets. The EEG-Report benchmark is constructed using data from two hospital sites in the Harvard Electroencephalography Database v4.1 (Zafar et al., 2025; Sun et al., 2025): Massachusetts General Hospital (MGH, S0001) and Brigham and Women's Hospital (BWH, S0002). In total, through our pipeline, we curated 12,290 clinical EEG reports matched to one or more EEG sessions from 10,886 patients. For model training and evaluation, we restrict our analysis to reports paired with a single EEG session.

□ **S0001:** This site includes diverse EEG visit types (routine EEG, epilepsy monitoring unit (EMU), portable EEG, complex EEG). We filtered only routine EEG and EMU samples paired with single sessions, excluding long recordings exceeding 10,000 seconds to prevent memory issues during training. We curated 5,049 reports from 4,669 patients.

□ **S0002:** From the available visit types (EEG, long-term monitoring, portable EEG), we retained only standard EEG visits with single corresponding sessions, yielding 4,873 reports from 4,379 patients.

For both sites, we performed patient-wise 60/20/20 splits into training, validation, and test sets. Additional dataset details are provided in Appendix A.

Baselines. As no existing EEG multimodal models with generative capabilities are available for EEG report generation, we establish baselines by augmenting local LLMs with EEG-derived inputs. We evaluate two settings: (1) Unimodal + text-only input, where the LLMs receive only clinical context as input without EEG data, providing a lower bound that quantifies hallucination and measures performance when the model does not attend to neural signals, and (2) Unimodal + text and EEG features input, where

Table 1. Report generation performance comparison on samples with clinical context across two hospital sites (S0001 and S0002). We evaluate BLEU-1, ROUGE-1, and METEOR under two input settings: (i) *Unimodal + Text Only Input*, where language models generate reports solely from clinical context text, and (ii) *Unimodal + Text + EEG Features Input*, where EEG-derived features are additionally provided. The table compares multiple strong baselines, including general-purpose and medical LLMs, against our CELM. The best results are highlighted in orange, and the best baseline per category is highlighted in blue. Relative improvements are also reported.

Method	S0001			S0002		
	BLEU-1	ROUGE-1	METEOR	BLEU-1	ROUGE-1	METEOR
Unimodal + Text Only Input						
Gemma-3-1b-it	0.1897 ± 0.1340	0.2112 ± 0.1408	0.1567 ± 0.1238	0.1509 ± 0.0898	0.2330 ± 0.0876	0.1319 ± 0.0565
Gemma-3n-e2b-it	0.1967 ± 0.1592	0.2410 ± 0.1722	0.1875 ± 0.1725	0.0925 ± 0.0769	0.2318 ± 0.0600	0.1181 ± 0.0472
Gemma-3-4b-it	0.2372 ± 0.1508	0.2857 ± 0.1590	0.2147 ± 0.1668	0.1538 ± 0.0990	0.2775 ± 0.0558	0.1506 ± 0.0514
Gemma-3n-e4b-it	0.1793 ± 0.1685	0.2416 ± 0.1778	0.1816 ± 0.1786	0.0539 ± 0.0664	0.1998 ± 0.0649	0.0993 ± 0.0490
MedGemma-4b-it	0.1502 ± 0.1725	0.2196 ± 0.1924	0.1529 ± 0.1835	0.0865 ± 0.0855	0.2280 ± 0.0734	0.1198 ± 0.0542
Llama-3.2-1b-instruct	0.0337 ± 0.0667	0.0919 ± 0.0744	0.0529 ± 0.0519	0.0340 ± 0.0700	0.0954 ± 0.0869	0.0494 ± 0.0504
Llama-3.2-3b-instruct	0.1951 ± 0.1630	0.2224 ± 0.1755	0.1843 ± 0.1864	0.1651 ± 0.1110	0.2346 ± 0.0877	0.1430 ± 0.0689
Llama-3.1-8b-instruct	0.2128 ± 0.1702	0.2511 ± 0.1872	0.1839 ± 0.1788	0.1629 ± 0.0970	0.2655 ± 0.0766	0.1480 ± 0.0581
Meta-llama-3-8b-instruct	0.2249 ± 0.1602	0.2673 ± 0.1731	0.1946 ± 0.1809	0.1441 ± 0.0847	0.2588 ± 0.0586	0.1416 ± 0.0481
Qwen3-1.7b	0.1335 ± 0.1481	0.1378 ± 0.1557	0.1102 ± 0.1316	0.0886 ± 0.1095	0.1189 ± 0.1296	0.0735 ± 0.0821
Qwen3-4b-instruct-2507	0.2795 ± 0.1243	0.3038 ± 0.1460	0.2418 ± 0.1440	0.1912 ± 0.0807	0.2690 ± 0.0448	0.1622 ± 0.0434
Unimodal + Text + EEG Features Input						
Gemma-3-1b-it	0.0068 ± 0.0442	0.0086 ± 0.0524	0.0064 ± 0.0462	0.0957 ± 0.0925	0.1755 ± 0.1157	0.0954 ± 0.0692
Gemma-3n-e2b-it	0.0083 ± 0.0504	0.0116 ± 0.0605	0.0088 ± 0.0543	0.0750 ± 0.0771	0.2190 ± 0.0840	0.1082 ± 0.0546
Gemma-3-4b-it	0.0085 ± 0.0532	0.0093 ± 0.0594	0.0078 ± 0.0558	0.2089 ± 0.0895	0.2886 ± 0.0458	0.1738 ± 0.0476
Gemma-3n-e4b-it	0.0101 ± 0.0348	0.0397 ± 0.0606	0.0231 ± 0.0392	0.0169 ± 0.0486	0.0357 ± 0.0903	0.0180 ± 0.0462
MedGemma-4b-it	0.1618 ± 0.1730	0.2100 ± 0.1919	0.1529 ± 0.1832	0.0888 ± 0.0910	0.1829 ± 0.1128	0.1000 ± 0.0702
Llama-3.2-1b-instruct	0.0310 ± 0.0615	0.0820 ± 0.0727	0.0473 ± 0.0479	0.0312 ± 0.0668	0.1016 ± 0.0773	0.0517 ± 0.0448
Llama-3.2-3b-instruct	0.1692 ± 0.1414	0.1844 ± 0.1611	0.1751 ± 0.1871	0.1779 ± 0.1101	0.2309 ± 0.0903	0.1540 ± 0.0743
Llama-3.1-8b-instruct	0.2040 ± 0.1450	0.2151 ± 0.1693	0.1844 ± 0.1647	0.1960 ± 0.0959	0.2256 ± 0.0904	0.1509 ± 0.0682
Qwen3-1.7b	0.2047 ± 0.1351	0.2051 ± 0.1453	0.1683 ± 0.1304	0.1890 ± 0.1048	0.2049 ± 0.1021	0.1413 ± 0.0724
Qwen3-4b-instruct-2507	0.1809 ± 0.0986	0.2058 ± 0.1192	0.2067 ± 0.1079	0.2483 ± 0.0425	0.2638 ± 0.0341	0.2017 ± 0.0285
CELM - SCC	0.3383 ± 0.1936	0.3843 ± 0.1876	0.2889 ± 0.1866	0.3767 ± 0.1557	0.4487 ± 0.1283	0.3232 ± 0.1261
CELM	0.4823 ± 0.1920	0.5565 ± 0.1683	0.4734 ± 0.1941	0.5695 ± 0.1702	0.6408 ± 0.1494	0.5597 ± 0.1728
Improvement	+72.56%	+83.18%	+95.78%	+129.36%	+122.04%	+177.49%

we augment the clinical context with channel-wise spectral band power features (delta, theta, alpha, beta, gamma) extracted from each EEG session, addressing context length limitation that prevents providing raw EEG arrays directly. We evaluate LLMs from three model families, including LLaMA-3 (Grattafiori et al., 2024), Gemma-3 (Team et al., 2025), and Qwen-3 (Yang et al., 2025), across multiple parameter scales. Additionally, we include MedGemma (Sellergren et al., 2025) as a medical LLM baseline. Additional implementation details are provided in Appendix B. We report smoothed BLEU-1 (Papineni et al., 2002), ROUGE-1 (Lin, 2004), and METEOR (Banerjee & Lavie, 2005) scores to evaluate report generation performance. Comprehensive results and metrics are provided in Appendix D.

5.1. Report Generation Performance Comparison

Table 1 compares CELM against unimodal baselines using either text-only or text with handcrafted EEG features as input, evaluated on test samples containing patient history. We report results for two CELM variants: **CELM-SCC**, which

uses sequence context compression to compress and produce a fixed number of projected EEG tokens, and **CELM**, which uses non-compressed EEG representations via sequence context alignment. When EEG features are provided, most baseline LLMs show modest improvements over text-only inputs on S0002 ($0.1912 \rightarrow 0.2483$), except LLaMA-3.1-8B, which fails due to its 8K token context limit. However, on S0001, performance degrades across baselines due to greater report complexity introduced by multiple sections.

Both CELM variants substantially outperform all baselines across all metrics, with CELM achieving the best results. On average, CELM yields a two-fold improvement over the strongest baseline across both sites and all evaluation metrics. For example, on the ROUGE score for S0002, performance improves from 0.2886 to 0.6408 relative to the strongest baseline. Although CELM-SCC outperforms the baselines, its performance gap relative to the non-compressed model (0.4487 vs 0.6408) underscores an important open challenge. This leads to an important future direction of developing efficient compression strategies

Table 2. Zero-context report generation performance on S0002. The best results are highlighted in orange, and the best baseline is highlighted in blue. Relative improvements are reported with respect to the strongest baseline under each setting.

Method	BLEU-1	ROUGE-1	METEOR
Unimodal + Text + EEG Features Input			
Gemma-3-1b-it	0.1019 ± 0.0782	0.1935 ± 0.0953	0.1052 ± 0.0556
Gemma-3n-2b-it	0.0717 ± 0.0710	0.2203 ± 0.0581	0.1116 ± 0.0411
Gemma-3-4b-it	0.1699 ± 0.0885	0.2557 ± 0.0484	0.1514 ± 0.0412
Gemma-3n-c4b-it	0.0058 ± 0.0304	0.0127 ± 0.0509	0.0067 ± 0.0281
Medgemma-4b-it	0.0559 ± 0.0660	0.1591 ± 0.0959	0.0820 ± 0.0520
Llama-3.2-1b-instruct	0.0265 ± 0.0627	0.1041 ± 0.0723	0.0530 ± 0.0396
Llama-3.2-3b-instruct	0.1261 ± 0.1028	0.1995 ± 0.0806	0.1214 ± 0.0617
Llama-3.1-8b-instruct	0.1556 ± 0.0817	0.2090 ± 0.0737	0.1298 ± 0.0506
Qwen3-1.7b	0.1772 ± 0.0999	0.1819 ± 0.0938	0.1304 ± 0.0688
Qwen3-4b-instruct-2507	0.2260 ± 0.0592	0.2315 ± 0.0501	0.1790 ± 0.0420
CELM - SCC	0.2991 ± 0.1276	0.3793 ± 0.0892	0.2574 ± 0.0891
CELM	0.4652 ± 0.1884	0.5248 ± 0.1869	0.4390 ± 0.1869
Improvement	+105.84%	+105.24%	+145.25%

—★ Gemma-3n-E4B —◇ Medgemma-4B —▲ Llama-3.1-8B —■ Qwen3-4B —● Ours

EEG Description/ Details

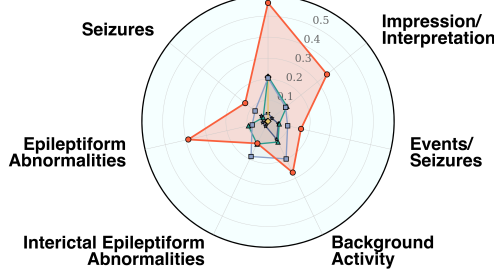


Figure 2. Section-wise comparison of report generation performance between CELM and the best-performing baselines from different LLM families.

that preserve clinically relevant information from long EEG sequences while remaining within LLM context constraints.

5.2. Zero-Context Report Generation

To assess our model’s ability to generate clinical reports solely from EEG signals, without relying on clinical context, we define a zero-context report generation task in which only EEG data is provided as input. This experiment also serves as a test of potential language-model bias, in which reports could be generated by inferring plausible clinical context while ignoring EEG inputs. We evaluate this task on a subset of the S0002 dataset containing reports without patient clinical context, and the results are summarized in Table 2. CELM significantly outperforms all baselines across all metrics, demonstrating that it effectively extracts and utilizes clinically relevant information from EEG recordings.

5.3. Performance Analysis by Report Section

Clinical EEG reports comprise multiple sections, each serving a distinct purpose: EEG description/details provides a detailed narrative of observed waveforms and patterns, impression/interpretation summarizes the clinical signifi-

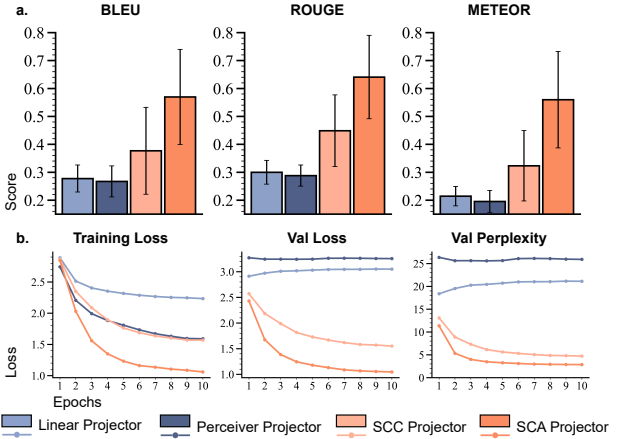


Figure 3. (a) Report generation performance of different projector variants. (b) Training dynamics of each variant, including training loss, validation loss, and perplexity curves.

cance of findings, background activity characterizes baseline rhythms, and events/seizures documents seizure episodes. To evaluate whether CELM can reliably generate these diverse sections, we conduct a section-wise analysis on S0001, which exhibits richer section diversity compared to S0002 (where reports predominantly contain only EEG description/details; see Figure 5 in Appendix). Figure 2 presents ROUGE-1 scores, comparing CELM against the best-performing unimodal baseline (text + EEG features) from each LLM family. CELM achieves the highest performance in 6 out of 7 report sections. Performance degrades in the interictal epileptiform abnormalities section, highlighting a key limitation and a challenge for ELMs in modeling rare and clinically complex events, an important direction for future work. Detailed results are provided in Table 12.

5.4. Alignment Module Ablation

The alignment module is a critical component of EEG-language models. In our initial experiments, we found that naive linear projection into the LLM embedding space is insufficient for the EEG domain. In this section, we present an ablation study comparing different alignment strategies. We evaluate two baseline alignment modules: (1) Linear projector, which directly maps EEG embeddings to the LLM embedding space using a single linear layer, and (2) Perceiver projector, which employs learnable query tokens that attend to EEG sequences via cross-attention followed by feedforward and projection. We compare these against our proposed SCA and SCC projectors, described in Section 4.3. Results are summarized in Figure 3.

As shown in Figure 3a, the SCA projector consistently achieves the best performance across all evaluation metrics. Analysis of training dynamics in Figure 3b further highlights the importance of modeling inter-epoch temporal dependencies prior to alignment. While the Linear and Per-

Qwen3-4B (Unimodal + Text + EEG Features)	Linear Projector	Ours	Ground Truth
<p>a. The EEG shows a predominantly normal background activity across all channels. Background rhythms are rhythmic and smooth, with no evidence of epileptiform discharges or abnormal slow waves. Delta (0.5-4-Hz) and theta (4-8-Hz) band power is within normal limits, with no significant deviations. Alpha (8-12-Hz) activity is present in the occipital regions, showing typical bilateral symmetry and normal amplitude. Beta (12-30-Hz) activity is present in all regions, with no focal or abnormal increases. Gamma (30-80-Hz) activity is minimal and within expected ranges. No evidence of sleep stages was observed, as the recording was ...</p> <p>b. The EEG findings are abnormal, indicating a generalized suppression of cortical activity. There is the absence of alpha and beta frequency bands, with prominent delta and theta activity. The marked reduction in gamma band power suggests impaired high-frequency cortical processing, which may be associated with cognitive deficits or altered consciousness. The overall pattern reflects a state of low cortical arousal and reduced brain function, which is concerning for a condition such as depression, chronic fatigue syndrome, or a ...</p>	<p>Background activity was characterized by a slow, bilateral, and asymmetrical beta rhythm with moderate high-voltage amplitudes in the 10-11 Hz range. There is predominantly over the central and parietal regions. The background activity was generally smooth, with no prominent epileptiform discharges or focal slowing. No significant physiologic variants were observed. Sleep stages were not evaluated due to the absence of sleep recording. No epileptiform discharges, such as spikes or sharp waves, were identified. The channels included in the recording (C3, C4, O1, O2, Cz, F3, F4, F7, F8, Fz, Fp1, Fp2, Fpz, P3, P4, Pz, T3, T4, T5, T6, A1, A2) ...</p> <p>The EEG findings are normal. Background activity is regular, symmetric, and with no detected abnormalities for a 35-year-old female. No epileptiform discharges, focal slowing, or other abnormalities were observed. The clinical context of no reported seizure history or neurological symptoms supports this interpretation. The EEG is consistent with a normal neurophysiologic status and does not indicate any underlying seizure disorder or significant brain pathology. ...</p>	<p>the waking background shows good organization, consisting of predominantly 30-40 v, 10-11 Hz power in the theta and delta range. there is moderate beta activity bilaterally. intermittent drowsiness is characterized by attenuation of the background, slow roving eye movements and bilateral slowing in the theta and delta range with shifting predominance, stage n2 sleep is not achieved. hyperventilation is not performed, photic stimulation results in mild bilateral driving responses. single lead ekg shows an apparent sinus rhythm of approximately 60-70 beats per minute. this routine ...</p> <p>this routine eeg, performed in the waking, drowsy and sleeping stages, was normal during the slow shifting bilaterally with shifting predominance and mild bilateral driving. these findings are consistent with mild to moderate generalized encephalopathy. ...</p>	<p>the waking background shows good organization, consisting of predominantly 30-40 v, 9-10 Hz posterior beta activity with no focal findings. there is moderate beta activity bilaterally. intermittent drowsiness is characterized by attenuation of the background, slow roving eye movements and bilateral slowing in the theta and delta range with shifting predominance, stage n2 sleep is not achieved. hyperventilation is not performed. photic stimulation results in mild bilateral driving at all flash frequencies. single lead ekg shows an apparent sinus rhythm of approximately 60-70 beats per minute. this ...</p> <p>impression: this routine eeg, performed in the waking, and excessive drowsiness state is abnormal because of 1) right fronto-central sharp transients (theta and delta transients that are somewhat periodic, at times, 2) right frontal delta slowing embedded within the **** rhythm, and 3) 2 suspicious sharp waves that are beyond what is expected for the known **** rhythm. taken together, these findings show underlying right frontal dysfunction with probable cortical irritability. there are no prior eegs available for ...</p>

Figure 4. Examples of generated reports on S0002. Comparisons between the unimodal baseline (text + EEG features), the linear-projector alignment variant, CELM, and the ground-truth reports. (a) EEG description/details; (b) Impression/interpretation.

ceiver projectors’ training losses decrease, their validation losses and perplexities increase, indicating overfitting. In contrast, both SCA and SCC exhibit more stable convergence, with lower validation loss and perplexity over time, and SCA converges faster across all variants. Notably, SCA achieves lower validation perplexity than other variants, indicating substantially higher confidence in token generation. Overall, this study confirms that modeling temporal dependencies between EEG epochs before projection is essential for effective EEG-to-language alignment.

5.5. Qualitative Analysis

Figure 4 presents qualitative comparisons on S0002 between the best-performing unimodal baseline (text with EEG features), the linear projector variant, and CELM, alongside ground truth reports. Figure 4a shows the EEG description/details section, while Figure 4b shows the impression/interpretation section. Across these examples, CELM produces reports that are more closely aligned with the ground truth, correctly identifying clinically relevant findings such as moderate bilateral beta activity, intermittent drowsiness, and bilateral slowing in the theta and delta ranges. In contrast, the linear projector and unimodal baselines fail to capture these. In the impression section, CELM identifies the recording as abnormal, whereas the linear projector variant incorrectly predicts it as normal. These results demonstrate the promise of ELMs in learning to generate clinical reports from unstructured notes paired with long EEG recordings. At the same time, they underscore the need for more rigorous and standardized benchmarking to assess these models. Additional examples spanning both sites, diverse report sections, and varying performance levels are provided in Appendix D.7 to further illustrate model strengths and failure modes.

6. Discussion and Implication

In this work, we demonstrate the feasibility of end-to-end clinical EEG–language modeling for generating structured reports directly from long-duration EEG recordings. The

strong performance gains over competitive baselines highlight the potential of ELMs for clinical report generation. However, several limitations remain. **Evaluation limitations.** ELM development is constrained by the lack of rigorous benchmarks and clinically grounded evaluation protocols, as common text generation metrics mainly capture lexical similarity rather than clinical correctness. **Memory scalability.** Memory remains a key bottleneck. While our approach supports EEG recordings of up to approximately 3 hours, further advances in memory-efficient representations are needed to scale to longer recordings. **Human-in-the-loop potential.** ELMs offer opportunities for human-in-the-loop workflows, where clinicians guide generation via targeted prompts instead of fixed templates, enabling better alignment with clinical intent.

7. Conclusion

We introduced CELM, the first clinical EEG-to-language foundation model for automated report generation from long-duration EEG recordings. CELM addresses three core challenges in this setting: (1) representing hour-scale EEG within LLM context limits via Epoch-Aggregated Tokenization, (2) preserving long-range temporal dependencies through Sequence-Aware Alignment, and (3) enabling flexible, multi-scale report generation via Prompt Fusion. We further presented a scalable EEG–Report benchmark construction pipeline and conducted extensive evaluations across hospital sites, report sections, and zero-context settings. Empirical results show that CELM consistently outperforms strong baselines. Overall, this work establishes EEG-to-language modeling as a distinct and promising research direction at the intersection of multimodal learning and clinical neurophysiology, and we hope that CELM and the accompanying benchmark construction pipeline will facilitate future advances in long-context EEG modeling and clinically grounded EEG language systems.

8. Impact Statement

This work advances machine learning research by introducing the first clinical EEG–language model that integrates long-duration clinical EEG signals with large language models to generate structured clinical reports. The proposed approach has the potential to support clinical workflows; however, this work is intended as a research contribution rather than a deployable clinical system. Any real-world application would require extensive validation, regulatory approval, and careful oversight by medical professionals. All data used in this study were deidentified by the dataset providers to protect participants’ protected health information (PHI). In addition, we strictly adhered to the data-use agreements and conducted all experiments using local large-language models.

References

Banerjee, S. and Lavie, A. Meteor: An automatic metric for mt evaluation with improved correlation with human judgments. In *Proceedings of the acl workshop on intrinsic and extrinsic evaluation measures for machine translation and/or summarization*, pp. 65–72, 2005.

Biswal, S., Xiao, C., Westover, M. B., and Sun, J. Eegtotext: learning to write medical reports from eeg recordings. In *Machine learning for healthcare conference*, pp. 513–531. PMLR, 2019.

Bordes, F., Pang, R. Y., Ajay, A., Li, A. C., Bardes, A., Petryk, S., Mañas, O., Lin, Z., Mahmoud, A., Jayaraman, B., Ibrahim, M., Hall, M., Xiong, Y., Lebensold, J., Ross, C., Jayakumar, S., Guo, C., Bouchacourt, D., Al-Tahan, H., Padthe, K., Sharma, V., Xu, H., Tan, X. E., Richards, M., Lavoie, S., Astolfi, P., Hemmat, R. A., Chen, J., Tirumala, K., Assouel, R., Moayeri, M., Talatof, A., Chaudhuri, K., Liu, Z., Chen, X., Garrido, Q., Ullrich, K., Agrawal, A., Saenko, K., Celikyilmaz, A., and Chandra, V. An introduction to vision-language modeling, 2024.

Döner, B., Ingolfsson, T. M., Benini, L., and Li, Y. Luna: Efficient and topology-agnostic foundation model for eeg signal analysis. *arXiv preprint arXiv:2510.22257*, 2025.

Duan, Y., Zhou, J., Wang, Z., Wang, Y.-K., and Lin, C.-t. Dewave: Discrete encoding of eeg waves for eeg to text translation. *Advances in Neural Information Processing Systems*, 36:9907–9918, 2023.

Gijsen, S. and Ritter, K. EEG-language pretraining for highly label-efficient clinical phenotyping. In *Forty-second International Conference on Machine Learning*, 2025.

Grattafiori, A., Dubey, A., Jauhri, A., Pandey, A., Kadian, A., Al-Dahle, A., Letman, A., Mathur, A., Schelten, A., Vaughan, A., et al. The llama 3 herd of models. *arXiv preprint arXiv:2407.21783*, 2024.

Herff, C., Heger, D., De Pesters, A., Telaar, D., Brunner, P., Schalk, G., and Schultz, T. Brain-to-text: decoding spoken phrases from phone representations in the brain. *Frontiers in neuroscience*, 8:141498, 2015.

Jaegle, A., Borgeaud, S., Alayrac, J.-B., Doersch, C., Ionescu, C., Ding, D., Koppula, S., Zoran, D., Brock, A., Shelhamer, E., et al. Perceiver io: A general architecture for structured inputs & outputs. *arXiv preprint arXiv:2107.14795*, 2021a.

Jaegle, A., Gimeno, F., Brock, A., Vinyals, O., Zisserman, A., and Carreira, J. Perceiver: General perception with iterative attention. In *International conference on machine learning*, pp. 4651–4664. PMLR, 2021b.

Jiang, W.-B., Zhao, L.-M., and Lu, B.-L. Large brain model for learning generic representations with tremendous eeg data in bci. *arXiv preprint arXiv:2405.18765*, 2024.

Katharopoulos, A., Vyas, A., Pappas, N., and Fleuret, F. Transformers are rnns: Fast autoregressive transformers with linear attention. In *International conference on machine learning*, pp. 5156–5165. PMLR, 2020.

Kostas, D., Aroca-Ouellette, S., and Rudzicz, F. Bendl: Using transformers and a contrastive self-supervised learning task to learn from massive amounts of eeg data. *Frontiers in Human Neuroscience*, 15:653659, 2021.

Kotoge, R., Chen, Z., Kimura, T., Matsubara, Y., Yanagisawa, T., Kishima, H., and Sakurai, Y. Evobrain: Dynamic multi-channel EEG graph modeling for time-evolving brain networks. In *The Thirty-ninth Annual Conference on Neural Information Processing Systems*, 2025.

Lee, W., Yang, J., Park, D., and Kim, Y. Automated clinical impression generation for medical signal data searches. *Applied Sciences*, 13(15), 2023.

Lin, C.-Y. ROUGE: A package for automatic evaluation of summaries. In *Text Summarization Branches Out*, pp. 74–81, 2004.

Liu, H., Li, C., Wu, Q., and Lee, Y. J. Visual instruction tuning. *Advances in neural information processing systems*, 36:34892–34916, 2023.

Makin, J. G., Moses, D. A., and Chang, E. F. Machine translation of cortical activity to text with an encoder–decoder framework. *Nature neuroscience*, 23(4):575–582, 2020.

Ndir, T. C., Schirrmeister, R. T., and Ball, T. Eeg-clip: Learning eeg representations from natural language descriptions. *Frontiers in Robotics and AI*, 12:1625731, 2025.

Ouahidi, Y. E., Lys, J., Thölke, P., Farrugia, N., Pasdeloup, B., Gripon, V., Jerbi, K., and Lioi, G. Reve: A foundation model for eeg—adapting to any setup with large-scale pretraining on 25,000 subjects. *arXiv preprint arXiv:2510.21585*, 2025.

Papineni, K., Roukos, S., Ward, T., and Zhu, W.-J. Bleu: a method for automatic evaluation of machine translation. In *Proceedings of the 40th annual meeting of the Association for Computational Linguistics*, pp. 311–318, 2002.

Pradeepkumar, J., Piao, X., Chen, Z., and Sun, J. Single-channel eeg tokenization through time-frequency modeling. *arXiv preprint arXiv:2502.16060*, 2025.

Radford, A., Kim, J. W., Hallacy, C., Ramesh, A., Goh, G., Agarwal, S., Sastry, G., Askell, A., Mishkin, P., Clark, J., et al. Learning transferable visual models from natural language supervision. In *International conference on machine learning*, pp. 8748–8763. PMLR, 2021.

Sellergren, A., Kazemzadeh, S., Jaroensri, T., Kiraly, A., Traverse, M., Kohlberger, T., Xu, S., Jamil, F., Hughes, C., Lau, C., et al. Medgemma technical report. *arXiv preprint arXiv:2507.05201*, 2025.

Shen, Y., Liu, Y., Zhu, J., Cao, X., Zhang, X., He, Y., Ye, W., Rehg, J. M., and Lourentzou, I. Fine-grained preference optimization improves spatial reasoning in VLMs. In *The Thirty-ninth Annual Conference on Neural Information Processing Systems*, 2025.

Sun, C., Jing, J., Turley, N., Alcott, C., Kang, W.-Y., Cole, A. J., Goldenholz, D. M., Lam, A., Amorim, E., Chu, C., et al. Harvard electroencephalography database: A comprehensive clinical electroencephalographic resource from four boston hospitals. *Epilepsia*, 2025.

Tatum IV, W. O., Selioutski, O., Ochoa, J. G., Clary, H. M., Cheek, J., Drislane, F. W., and Tsuchida, T. N. American clinical neurophysiology society guideline 7: guidelines for eeg reporting. *The Neurodiagnostic Journal*, 56(4): 285–293, 2016.

Team, G., Kamath, A., Ferret, J., Pathak, S., Vieillard, N., Merhej, R., Perrin, S., Matejovicova, T., Ramé, A., Rivière, M., et al. Gemma 3 technical report. *arXiv preprint arXiv:2503.19786*, 2025.

Wang, G., Liu, W., He, Y., Xu, C., Ma, L., and Li, H. Eegpt: Pretrained transformer for universal and reliable representation of eeg signals. *Advances in Neural Information Processing Systems*, 37:39249–39280, 2024a.

Wang, J., Zhao, S., Luo, Z., Zhou, Y., Jiang, H., Li, S., Li, T., and Pan, G. Cbramod: A criss-cross brain foundation model for eeg decoding. *arXiv preprint arXiv:2412.07236*, 2024b.

Wang, S., Li, B. Z., Khabsa, M., Fang, H., and Ma, H. Linformer: Self-attention with linear complexity. *arXiv preprint arXiv:2006.04768*, 2020.

Wang, Z. and Ji, H. Open vocabulary electroencephalography-to-text decoding and zero-shot sentiment classification. In *Proceedings of the AAAI Conference on Artificial Intelligence*, volume 36, pp. 5350–5358, 2022.

Willett, F. R., Kunz, E. M., Fan, C., Avansino, D. T., Wilson, G. H., Choi, E. Y., Kamdar, F., Glasser, M. F., Hochberg, L. R., Druckmann, S., et al. A high-performance speech neuroprosthesis. *Nature*, 620(7976):1031–1036, 2023.

Yang, A., Li, A., Yang, B., Zhang, B., Hui, B., Zheng, B., Yu, B., Gao, C., Huang, C., Lv, C., et al. Qwen3 technical report. *arXiv preprint arXiv:2505.09388*, 2025.

Yang, C., Westover, M., and Sun, J. Biot: Biosignal transformer for cross-data learning in the wild. *Advances in Neural Information Processing Systems*, 36:78240–78260, 2023.

Yin, K. and Shin, H.-B. Neurolex: A lightweight domain language model for eeg report understanding and generation. *10.48550/arXiv.2511.12851*, 2025.

Zafar, S., Loddenkemper, T., Lee, J., Cole, A., Goldenholz, D., Peters, J., Lam, A., Amorim, E., Chu, C., Cash, S., et al. Harvard electroencephalography database (version 4.1). *Brain Data Science Platform*, 2025.

Zhou, J., Duan, Y., Chang, F., Do, T., Wang, Y.-K., and Lin, C.-T. Belt-2: Bootstrapping eeg-to-language representation alignment for multi-task brain decoding. *arXiv preprint arXiv:2409.00121*, 2024.

Appendix

A. Details of EEG-Report Benchmark

This section provides detailed information on the EEG-Report benchmark constructed in our study. Table 3 summarizes key statistics, including the number of EEG-report pairs, patient counts, and total EEG recording duration for each site. Figure 5 further illustrates dataset distributions across EEG session duration, patient demographics (age and gender), and EEG report sections.

Table 3. Statistics of the EEG-Report benchmark.

Site	# of Paired EEG & Reports	# of Patients	Total Duration (hrs)
S0001	5049	4669	6639
S0002	4873	4379	4367

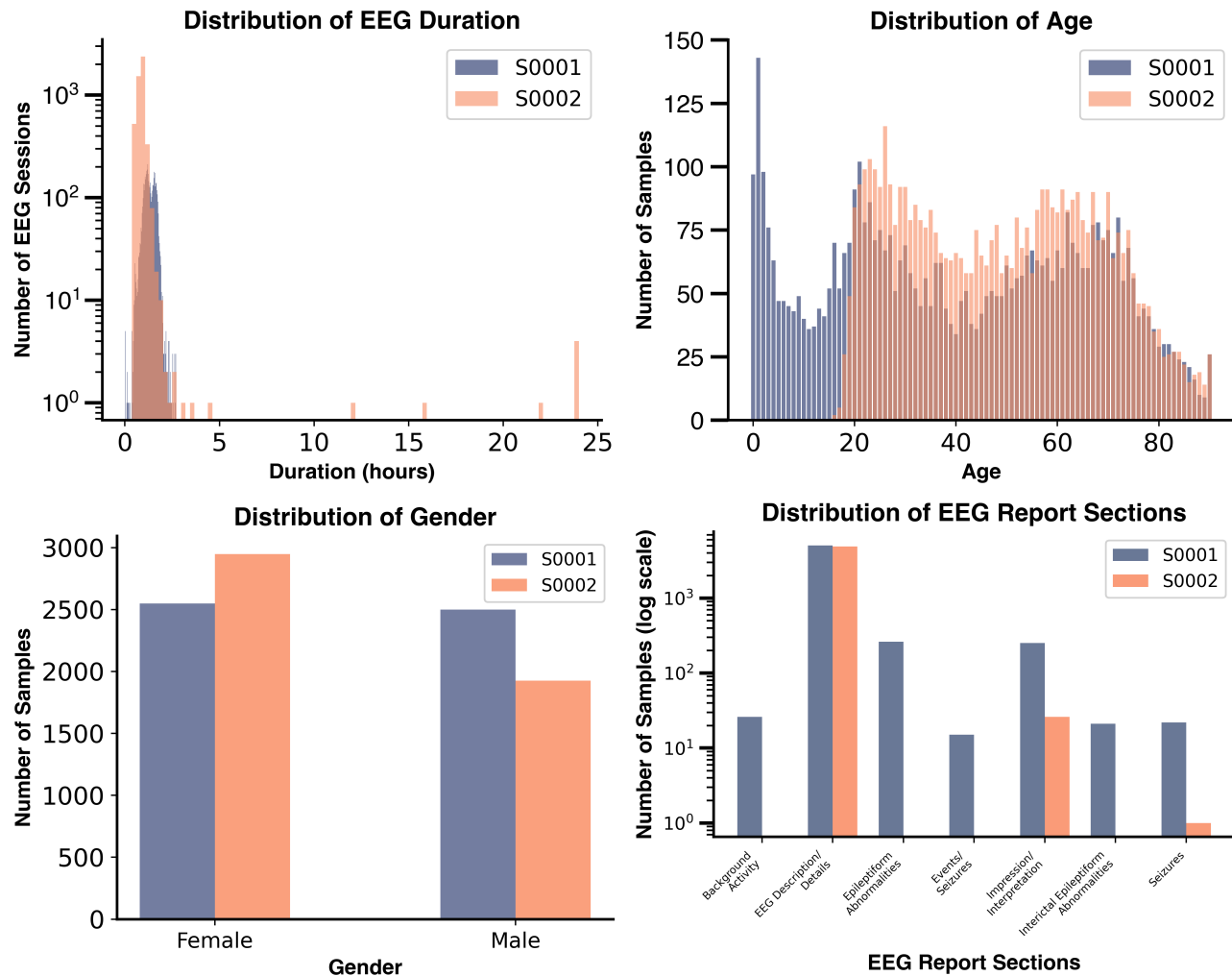


Figure 5. Dataset statistics of the filtered and constructed EEG-Report Benchmark used in our study

B. Additional Experiment Details

B.1. Band Power Features

This section describes the extraction of handcrafted EEG features used in the unimodal text + EEG feature baselines. To construct EEG features that fit current context-length constraints, we extract band-power features from EEG recordings. For each 10-second multichannel EEG segment, we compute channel-wise band power using Welch’s method by first estimating the power spectral density and then integrating it within five EEG frequency bands: delta (0.5–4 Hz), theta (4–8 Hz), alpha (8–13 Hz), beta (13–30 Hz), and gamma (30–80 Hz). To further reduce input sequence length for LLMs with limited context windows, we optionally pool consecutive epochs by concatenating their time axes prior to spectral estimation, yielding a more compact representation. The resulting band power values are formatted as structured text and provided as input to the LLMs (see example in Figure 7).

B.2. Evaluation Metrics

We evaluate report generation performance using a comprehensive set of natural language generation metrics to evaluate different aspects of generation quality. In the main manuscript, we report smoothed BLEU-1, ROUGE-1, and METEOR scores. In Appendix D, we additionally report smoothed BLEU-4, ROUGE-2, ROUGE-L, and ROUGE-LSUM. We further include per-sample score distributions for all metrics in Appendix D.5.

B.3. Baselines and Prompts

In this section, we provide additional details on the baseline models and the prompts used in our experiments. Table 4 summarizes all LLMs considered in our study along with their respective context lengths¹, further underscoring the practical challenges of directly conditioning LLMs on long-duration EEG recordings. Figures 6 and 7 present the prompts used for the unimodal text-only and unimodal text + EEG feature baselines, respectively. For clarity, we provide examples for certain prompt sections using bounding boxes.

Table 4. Summary of LLM Baselines

LLM	Family	Context Length
Gemma-3-1b-it	Gemma 3	32K
Gemma-3n-E2B-it	Gemma 3	32K
Gemma-3n-E4B-it	Gemma 3	32K
Gemma-3-4b-it	Gemma 3	128K
Medgemma-4b-it	Gemma	128K
Llama-3.2-1B-Instruct	Llama-3.2	128K
Llama-3.2-3B-Instruct	Llama-3.2	128K
Llama-3.1-8B-Instruct	Llama-3.1	128K
Meta-Llama-3-8B-Instruct	Llama-3	8K
Qwen3-1.7B	Qwen 3	32K
Qwen3-4B-Instruct-2507	Qwen 3	256K

¹Context length information is extracted from their respective technical reports and Hugging Face <https://huggingface.co/>

Unimodal + Text Only Prompt

You are an expert clinical neurophysiologist specializing in EEG interpretation and clinical report generation.

TASK

Your task is to generate the specified sections of a formal clinical EEG report using only the provided:

- Patient history
- EEG description

EEG SECTION DESCRIPTIONS

[STANDARDIZED_SECTION_DESCRIPTIONS]

e.g. EEG DESCRIPTION/DETAILS: Detailed narrative of EEG findings including background activity, sleep stages, physiologic variants, and abnormalities observed during the recording period.

GUIDELINES

- Generate only the sections listed in **SECTIONS TO BE GENERATED**.
- Do NOT generate any additional sections.
- Do NOT repeat the same section more than once.
- Only generate the output in the JSON format and do not include any other text or explanation.

OUTPUT FORMAT (STRICT)

Return ONLY the following JSON structure, with no preamble, explanation, or markdown:

```
json
{"report_sections": [
  {"section_name": "Name of the section as given in SECTIONS TO BE
  GENERATED",
   "section_text": "Generated text for the section in string"},
  ...
]}
```

SECTIONS TO BE GENERATED

[SECTION_NAMES]

e.g. ['EEG DESCRIPTION/DETAILS']

PATIENT HISTORY AND EEG DESCRIPTION

[PATIENT_HISTORY_AND_EEG_DESCRIPTION]

e.g. age: 77.0, gender: Female, indication: ***** y.o. female with history of afib, l mca stroke, and headaches, presenting with episodes of altered consciousness concerning for seizure vs. syncope.
none pertinent medications: keppra, neurontin, seroquel. none

Now generate the EEG report.

Figure 6. Prompt for unimodal + text only baselines.

Unimodal + Text + EEG Features Prompt**EEG-DERIVED STATISTICS**

```
{"eeg_session_0": {"delta (0.5-4Hz) band power (dB)": [[-22.90, -21.60, -22.20, ...]], "theta (4-8Hz) band power (dB)": [[-25.30, -24.80, -24.50, ...]], "alpha (8-12Hz) band power (dB)": [[-27.50, -26.60, -27.30, ...]], "beta (12-30Hz) band power (dB)": [[-30.60, -30.20, -30.70, ...]], "gamma (30-80Hz) band power (dB)": [[-36.30, -36.10, -36.30, ...]]},
```

EEG CHANNELS

```
['C3', 'C4', 'O1', 'O2', 'Cz', 'F3', 'F4', 'F7', 'F8', 'Fz', 'Fp1', 'Fp2', 'Fpz', 'P3', 'P4', 'Pz', 'T3', 'T4', 'T5', 'T6', 'A1', 'A2']
```

You are an expert clinical neurophysiologist specializing in EEG interpretation and clinical report generation.

TASK

Your task is to generate the specified sections of a formal clinical EEG report using only the provided:

- Patient history
- EEG description
- EEG Channels
- EEG-derived statistics (provided above)

EEG SECTION DESCRIPTIONS**[STANDARDIZED_SECTION_DESCRIPTIONS]**

e.g. EEG DESCRIPTION/DETAILS: Detailed narrative of EEG findings including background activity, sleep stages, physiologic variants, and abnormalities observed during the recording period.

GUIDELINES

- Generate only the sections listed in **SECTIONS TO BE GENERATED**.
- Do NOT generate any additional sections.
- Do NOT repeat the same section more than once.
- Only generate the output in the JSON format and do not include any other text or explanation.

OUTPUT FORMAT (STRICT)

Return ONLY the following JSON structure, with no preamble, explanation, or markdown:

```
json
{"report_sections": [
  {"section_name": "Name of the section as given in SECTIONS TO BE GENERATED",
   "section_text": "Generated text for the section in string"}, ...
]}
```

SECTIONS TO BE GENERATED**[SECTION_NAMES]**

e.g. ['EEG DESCRIPTION/DETAILS']

PATIENT HISTORY AND EEG DESCRIPTION**[PATIENT_HISTORY_AND_EEG_DESCRIPTION]**

e.g. age: 77.0, gender: Female, indication: ***** y.o. female with history of afib, 1 mca stroke, and headaches, presenting with episodes of altered consciousness concerning for seizure vs. syncope.
none pertinent medications: keppra, neurontin, seroquel. none

Now generate the EEG report.

Figure 7. Prompt for unimodal + text and EEG features as input baselines.

C. Implementation Details

To facilitate reproducibility, we provide the complete source code for constructing the EEG-report benchmark from the Harvard Electroencephalography Database and the EHR database hosted on the Brain Data Science Platform, together with our model implementation, training scripts, data loaders, and pretrained weights at <https://anonymous.4open.science/r/CELM-3AF4>. Additionally, we provide the detailed implementation details of our approach in this section and the prompts used for the baselines in Appendix B. The dataset utilized for this study is publicly available and can be accessed at <https://bdsp.io/content/harvard-eeg-db/4.1/> after obtaining credentialed access.

C.1. Model Details and Hyperparameters

We use CBraMod (Wang et al., 2024b) as the EEG encoder and Qwen-4B-Instruct-2507 as the local LLM backbone in our framework. CBraMod is selected due to its SOTA performance among EEG foundation models and its pretraining on large, diverse EEG datasets. In addition, our encoder ablation study comparing CBraMod with LaBraM shows that CBraMod consistently achieves better performance. We chose Qwen-4B-Instruct-2507 as the LLM backbone because it outperforms other local LLMs in unimodal baselines and reliably follows instruction prompts to generate outputs with the required structure. In Table 5, we provide the hyperparameters of the alignment modules used in our study.

Table 5. Hyperparameters of the alignment (projector) modules.

Module	Hyperparameter	Values
Linear Projector	Projector Input Dimension (CBraMod Embedding Dimension)	200
	Projector Output Dimension (Qwen-3 4B Embedding Dimension)	2560
	Bias	True
	# Trainable parameters	522,240
Perceiver Projector	# Query tokens	256
	Embedding Dimension	200
	# Attention heads	8
	# Perceiver layers (cross attention followed by feed-forward layer)	2
	Dropout	0.1
	Feed-forward multiplier (\times)	2
	Final linear projection	Linear(200, 2560)
Sequence Context Compression (SCC)	# Trainable parameters	1,219,040
	Transformer Encoder Type	Linear attention transformer
	Transformer # heads	8
	Transformer # layers (depth)	1
	# Query tokens	256
Sequence Context Alignment (SCA)	# Perceiver layers	1
	# Trainable parameters	1,378,440
	Transformer Encoder Type	Linear attention transformer
	# Heads	8
Sequence Context Alignment (SCA)	# Transformer Layers	2
	Final linear projection	Linear(200, 2560)
	# Trainable parameters	1,486,240

C.2. Training Details

In our approach, the EEG encoder and LLM backbone are frozen, and only the alignment module is trained via supervised learning using a next-token prediction objective. Training details are summarized in Table 6.

C.3. Prompts

Figure 8 illustrates the prompt used in our approach along with the EEG tokens. We also provide examples of the sections in the prompt.

Table 6. Training details

Hyperparameter	Values
Batch size	4
Gradient accumulation steps	4
Optimizer	AdamW
Learning rate	1e-4
Weight decay	0.01
β_1	0.9
β_2	0.99
LR scheduler	Linear scheduler with warmup
# of training epochs	10
Warm-up ratio	0.1
Mixed precision	bf16

ELM Prompt

Input : EEG projected tokens prepended to text tokens.

EEG CHANNELS

```
['C3', 'C4', 'O1', 'O2', 'Cz', 'F3', 'F4', 'F7', 'F8', 'Fz', 'Fp1', 'Fp2', 'Fpz',  
'P3', 'P4', 'Pz', 'T3', 'T4', 'T5', 'T6', 'A1', 'A2']
```

You are an expert clinical neurophysiologist specializing in EEG interpretation and clinical report generation.

TASK

Your task is to generate the specified sections (**SECTIONS TO BE GENERATED**) of a formal clinical EEG report using the above provided data of EEG recording sessions and the following information:

- Patient history
- EEG description
- EEG Channels

EEG SECTION DESCRIPTIONS

[STANDARDIZED_SECTION_DESCRIPTIONS]

e.g. EEG DESCRIPTION/DETAILS: Detailed narrative of EEG findings including background activity, sleep stages, physiologic variants, and abnormalities observed during the recording period.

GUIDELINES

- Generate only the sections listed in **SECTIONS TO BE GENERATED**.
- Do NOT generate any additional sections.
- Do NOT repeat the same section more than once.
- Only generate the output in the JSON format and do not include any other text or explanation.

OUTPUT FORMAT (STRICT)

Return ONLY the following JSON structure, with no preamble, explanation, or markdown:

```
json  
{"report_sections": [  
    {"section_name": "Name of the section as given in SECTIONS TO BE  
    GENERATED",  
    "section_text": "Generated text for the section in string"},  
    ... ]}
```

SECTIONS TO BE GENERATED

[SECTION_NAMES]

e.g. ['EEG DESCRIPTION/DETAILS']

PATIENT HISTORY AND EEG DESCRIPTION

[PATIENT_HISTORY_AND_EEG_DESCRIPTION]

e.g. age: 77.0, gender: Female, indication: ***** y.o. female with history of afib, 1 mca stroke, and headaches, presenting with episodes of altered consciousness concerning for seizure vs. syncope.
none pertinent medications: keppra, neurontin, seroquel. none

Now generate the EEG report.

Figure 8. Prompt for CELM.

D. Additional Experiment Results

D.1. Extended Report Generation Performance on S0001

Table 7 presents a comprehensive performance comparison of EEG report generation on the S0001 site for samples with clinical context. Both proposed variants consistently outperform all baselines across all evaluation metrics. Among them, CELM achieves better performance compared to the memory-efficient CELM -SCC variant across all metrics.

Table 7. Report generation performance comparison on samples with clinical context on S0001. We provide results for a complete set of evaluation metrics under two input settings: (i) *Unimodal + Text Only Input*, where language models generate reports solely from clinical context text, and (ii) *Unimodal + Text + EEG Features Input*, where EEG-derived features are additionally provided. The table compares multiple strong baselines, including general-purpose and medical LLMs, against our CELM. The best results are highlighted in orange, and the best baseline per category is highlighted in blue.

Method	BLEU-1	BLEU-4	ROUGE-1	ROUGE-2	ROUGE-L	ROUGE-LSUM	BERTScore	METEOR
Unimodal + Text Only Input								
Gemma-3-1b-it	0.1897 ± 0.1340	0.0351 ± 0.0694	0.2112 ± 0.1408	0.0431 ± 0.0985	0.1356 ± 0.1129	0.1381 ± 0.1137	0.6461 ± 0.3014	0.1567 ± 0.1238
Gemma-3n-e2b-it	0.1967 ± 0.1592	0.0641 ± 0.1402	0.2410 ± 0.1722	0.0702 ± 0.1939	0.1657 ± 0.1826	0.1687 ± 0.1824	0.7848 ± 0.0765	0.1875 ± 0.1725
Gemma-3-4b-it	0.2372 ± 0.1508	0.0641 ± 0.1349	0.2857 ± 0.1590	0.0821 ± 0.1893	0.1893 ± 0.1749	0.1929 ± 0.1747	0.7941 ± 0.0922	0.2147 ± 0.1668
Gemma-3n-e4b-it	0.1793 ± 0.1685	0.0642 ± 0.1486	0.2416 ± 0.1778	0.0763 ± 0.2003	0.1659 ± 0.1892	0.1687 ± 0.1890	0.7847 ± 0.0747	0.1816 ± 0.1786
Medgemma-4b-it	0.1502 ± 0.1725	0.0485 ± 0.1383	0.2196 ± 0.1924	0.0654 ± 0.1954	0.1569 ± 0.1908	0.1593 ± 0.1910	0.6683 ± 0.2994	0.1529 ± 0.1835
Llama-3.2-1b-instruct	0.0337 ± 0.0667	0.0059 ± 0.0166	0.0919 ± 0.0744	0.0053 ± 0.0217	0.0615 ± 0.0500	0.0629 ± 0.0515	0.5580 ± 0.3284	0.0529 ± 0.0519
Llama-3.2-3b-instruct	0.1951 ± 0.1630	0.0625 ± 0.1487	0.2224 ± 0.1755	0.0669 ± 0.1860	0.1511 ± 0.1760	0.1550 ± 0.1759	0.7116 ± 0.2311	0.1843 ± 0.1864
Llama-3.1-8b-instruct	0.2128 ± 0.1702	0.0598 ± 0.1444	0.2511 ± 0.1872	0.0753 ± 0.1967	0.1689 ± 0.1889	0.1722 ± 0.1892	0.6994 ± 0.2605	0.1839 ± 0.1788
Meta-llama-3-8b-instruct	0.2249 ± 0.1602	0.0620 ± 0.1418	0.2673 ± 0.1731	0.0765 ± 0.1895	0.1758 ± 0.1785	0.1795 ± 0.1787	0.7392 ± 0.2055	0.1946 ± 0.1809
Qwen3-1.7b	0.1335 ± 0.1481	0.0213 ± 0.0450	0.1378 ± 0.1557	0.0285 ± 0.0704	0.0835 ± 0.1054	0.0855 ± 0.1075	0.3856 ± 0.3941	0.1102 ± 0.1316
Qwen3-4b-instruct-2507	0.2795 ± 0.1243	0.0593 ± 0.1100	0.3038 ± 0.1460	0.0763 ± 0.1672	0.1872 ± 0.1623	0.1916 ± 0.1622	0.7975 ± 0.0852	0.2418 ± 0.1440
Unimodal + Text + EEG Features Input								
Gemma-3-1b-it	0.0068 ± 0.0442	0.0019 ± 0.0273	0.0086 ± 0.0524	0.0022 ± 0.0367	0.0063 ± 0.0449	0.0064 ± 0.0451	0.0311 ± 0.1512	0.0064 ± 0.0462
Gemma-3n-e2b-it	0.0083 ± 0.0504	0.0029 ± 0.0330	0.0116 ± 0.0605	0.0032 ± 0.0403	0.0080 ± 0.0500	0.0083 ± 0.0507	0.0415 ± 0.1756	0.0088 ± 0.0543
Gemma-3-4b-it	0.0085 ± 0.0532	0.0025 ± 0.0299	0.0093 ± 0.0594	0.0032 ± 0.0402	0.0062 ± 0.0466	0.0065 ± 0.0474	0.0247 ± 0.1384	0.0078 ± 0.0558
Gemma-3n-e4b-it	0.0101 ± 0.0348	0.0020 ± 0.0067	0.0397 ± 0.0606	0.0014 ± 0.0072	0.0259 ± 0.0395	0.0262 ± 0.0401	0.2498 ± 0.3570	0.0231 ± 0.0392
Medgemma-4b-it	0.1618 ± 0.1730	0.0488 ± 0.1400	0.2100 ± 0.1919	0.0611 ± 0.1870	0.1455 ± 0.1858	0.1482 ± 0.1862	0.6172 ± 0.3319	0.1529 ± 0.1832
Llama-3.2-1b-instruct	0.0310 ± 0.0615	0.0053 ± 0.0119	0.0820 ± 0.0727	0.0037 ± 0.0150	0.0547 ± 0.0485	0.0556 ± 0.0493	0.4978 ± 0.3562	0.0473 ± 0.0479
Llama-3.2-3b-instruct	0.1692 ± 0.1414	0.0528 ± 0.1147	0.1844 ± 0.1611	0.0543 ± 0.1575	0.1271 ± 0.1529	0.1342 ± 0.1536	0.6441 ± 0.2898	0.1751 ± 0.1871
Llama-3.1-8b-instruct	0.2040 ± 0.1450	0.0508 ± 0.1177	0.2151 ± 0.1693	0.0617 ± 0.1695	0.1469 ± 0.1690	0.1499 ± 0.1693	0.6930 ± 0.2289	0.1844 ± 0.1647
Qwen3-1.7b	0.2047 ± 0.1351	0.0331 ± 0.0611	0.2051 ± 0.1453	0.0422 ± 0.0971	0.1286 ± 0.1150	0.1317 ± 0.1163	0.6063 ± 0.3215	0.1683 ± 0.1304
Qwen3-4b-instruct-2507	0.1809 ± 0.0986	0.0288 ± 0.0555	0.2058 ± 0.1192	0.0402 ± 0.0969	0.1275 ± 0.1082	0.1303 ± 0.1087	0.7249 ± 0.1840	0.2067 ± 0.1079
CELM-SCC	0.3383 ± 0.1936	0.1345 ± 0.1860	0.3843 ± 0.1876	0.1651 ± 0.1960	0.2699 ± 0.1867	0.2732 ± 0.1865	0.7949 ± 0.1783	0.2889 ± 0.1866
CELM	0.4823 ± 0.1920	0.2831 ± 0.1952	0.5565 ± 0.1683	0.3458 ± 0.2036	0.4687 ± 0.1857	0.4702 ± 0.1852	0.8697 ± 0.0901	0.4734 ± 0.1941

D.2. Extended Report Generation Performance on S0002

Tables 8 and 9 present a comprehensive performance comparison of EEG report generation on the S0002 site under settings with and without patient clinical context. Both proposed variants consistently outperform all baselines across all evaluation metrics. Among them, CELM achieves better performance compared to the memory-efficient CELM -SCC variant across all metrics, except for BERTScore in the zero-context setting.

Table 8. Report generation performance comparison on samples with clinical context on S0002. We provide results for a complete set of evaluation metrics under two input settings: (i) *Unimodal + Text Only Input*, where language models generate reports solely from clinical context text, and (ii) *Unimodal + Text + EEG Features Input*, where EEG-derived features are additionally provided. The table compares multiple strong baselines, including general-purpose and medical LLMs, against our CELM. The best results are highlighted in orange, and the best baseline per category is highlighted in blue.

Method	BLEU-1	BLEU-4	ROUGE-1	ROUGE-2	ROUGE-L	ROUGE-LSUM	BERTScore	METEOR
Unimodal + Text Only Input								
Gemma-3-1b-it	0.1509 ± 0.0898	0.0158 ± 0.0121	0.2330 ± 0.0876	0.0302 ± 0.0210	0.1233 ± 0.0467	0.1259 ± 0.0495	0.7058 ± 0.2423	0.1319 ± 0.0565
Gemma-3n-e2b-it	0.0925 ± 0.0769	0.0115 ± 0.0230	0.2318 ± 0.0600	0.0274 ± 0.0346	0.1224 ± 0.0377	0.1254 ± 0.0408	0.7683 ± 0.0560	0.1181 ± 0.0472
Gemma-3-4b-it	0.1538 ± 0.0990	0.0163 ± 0.0180	0.2775 ± 0.0558	0.0354 ± 0.0335	0.1407 ± 0.0336	0.1440 ± 0.0369	0.7851 ± 0.0730	0.1506 ± 0.0514
Gemma-3n-e4b-it	0.0539 ± 0.0664	0.0083 ± 0.0243	0.1998 ± 0.0649	0.0281 ± 0.0358	0.1152 ± 0.0392	0.1175 ± 0.0407	0.7635 ± 0.0525	0.0993 ± 0.0490
Medgemma-4b-it	0.0865 ± 0.0855	0.0109 ± 0.0194	0.2280 ± 0.0734	0.0341 ± 0.0341	0.1315 ± 0.0433	0.1345 ± 0.0458	0.7576 ± 0.1375	0.1198 ± 0.0542
Llama-3.2-1b-instruct	0.0340 ± 0.0700	0.0036 ± 0.0073	0.0954 ± 0.0869	0.0082 ± 0.0135	0.0581 ± 0.0483	0.0596 ± 0.0509	0.5139 ± 0.3501	0.0494 ± 0.0504
Llama-3.2-3b-instruct	0.1651 ± 0.1110	0.0186 ± 0.0256	0.2346 ± 0.0877	0.0321 ± 0.0351	0.1221 ± 0.0478	0.1271 ± 0.0517	0.7261 ± 0.1919	0.1430 ± 0.0689
Llama-3.1-8b-instruct	0.1629 ± 0.0970	0.0190 ± 0.0237	0.2655 ± 0.0766	0.0424 ± 0.0356	0.1368 ± 0.0444	0.1404 ± 0.0476	0.7502 ± 0.1531	0.1480 ± 0.0581
Meta-llama-3-8b-instruct	0.1441 ± 0.0847	0.0176 ± 0.0232	0.2588 ± 0.0586	0.0403 ± 0.0330	0.1354 ± 0.0374	0.1390 ± 0.0411	0.7702 ± 0.0817	0.1416 ± 0.0481
Qwen3-1.7b	0.0886 ± 0.1095	0.0097 ± 0.0124	0.1189 ± 0.1296	0.0142 ± 0.0191	0.0633 ± 0.0686	0.0652 ± 0.0716	0.3650 ± 0.3893	0.0735 ± 0.0821
Qwen3-4b-instruct-2507	0.1912 ± 0.0807	0.0218 ± 0.0197	0.2690 ± 0.0448	0.0398 ± 0.0298	0.1317 ± 0.0295	0.1350 ± 0.0324	0.7867 ± 0.0178	0.1622 ± 0.0434
Unimodal + Text + EEG Features Input								
Gemma-3-1b-it	0.0957 ± 0.0925	0.0109 ± 0.0203	0.1755 ± 0.1157	0.0239 ± 0.0316	0.0980 ± 0.0653	0.1007 ± 0.0684	0.5785 ± 0.3384	0.0954 ± 0.0692
Gemma-3n-e2b-it	0.0750 ± 0.0771	0.0093 ± 0.0226	0.2190 ± 0.0840	0.0350 ± 0.0350	0.1256 ± 0.0516	0.1281 ± 0.0539	0.7175 ± 0.2153	0.1082 ± 0.0546
Gemma-3-4b-it	0.2089 ± 0.0895	0.0222 ± 0.0186	0.2886 ± 0.0458	0.0446 ± 0.0331	0.1451 ± 0.0315	0.1491 ± 0.0356	0.7883 ± 0.0418	0.1738 ± 0.0476
Gemma-3n-e4b-it	0.0169 ± 0.0486	0.0018 ± 0.0052	0.0357 ± 0.0903	0.0049 ± 0.0138	0.0194 ± 0.0490	0.0207 ± 0.0526	0.1073 ± 0.2678	0.0180 ± 0.0462
Medgemma-4b-it	0.0888 ± 0.0910	0.0110 ± 0.0195	0.1829 ± 0.1128	0.0248 ± 0.0349	0.1008 ± 0.0641	0.1029 ± 0.0660	0.5979 ± 0.3260	0.1000 ± 0.0702
Llama-3.2-1b-instruct	0.0312 ± 0.0668	0.0035 ± 0.0073	0.1016 ± 0.0773	0.0090 ± 0.0142	0.0620 ± 0.0420	0.0634 ± 0.0438	0.5903 ± 0.3062	0.0517 ± 0.0448
Llama-3.2-3b-instruct	0.1779 ± 0.1101	0.0207 ± 0.0224	0.2309 ± 0.0903	0.0350 ± 0.0349	0.1217 ± 0.0484	0.1364 ± 0.0575	0.7377 ± 0.1557	0.1540 ± 0.0743
Llama-3.1-8b-instruct	0.1960 ± 0.0959	0.0227 ± 0.0251	0.2256 ± 0.0904	0.0365 ± 0.0364	0.1198 ± 0.0542	0.1236 ± 0.0574	0.6895 ± 0.2171	0.1509 ± 0.0682
Qwen3-1.7b	0.1890 ± 0.1048	0.0185 ± 0.0118	0.2049 ± 0.1021	0.0236 ± 0.0179	0.1077 ± 0.0530	0.1110 ± 0.0568	0.6345 ± 0.2944	0.1413 ± 0.0724
Qwen3-4b-instruct-2507	0.2483 ± 0.0425	0.0217 ± 0.0098	0.2638 ± 0.0341	0.0334 ± 0.0179	0.1283 ± 0.0180	0.1322 ± 0.0250	0.7704 ± 0.0125	0.2017 ± 0.0285
CELM-SCC	0.3767 ± 0.1557	0.1671 ± 0.1054	0.4487 ± 0.1283	0.2149 ± 0.1109	0.3232 ± 0.1263	0.3268 ± 0.1258	0.8229 ± 0.1341	0.3232 ± 0.1261
CELM	0.5695 ± 0.1702	0.4145 ± 0.1639	0.6408 ± 0.1494	0.4805 ± 0.1603	0.5757 ± 0.1624	0.5772 ± 0.1613	0.8755 ± 0.1521	0.5597 ± 0.1728

Table 9. Zero-context report generation performance on S0002. The best results are highlighted in orange, and the best baseline is highlighted in blue.

Method	BLEU-1	BLEU-4	ROUGE-1	ROUGE-2	ROUGE-L	ROUGE-LSUM	BERTScore	METEOR
Unimodal + Text + EEG Features Input								
Gemma-3-1b-it	0.1019 ± 0.0782	0.0105 ± 0.0082	0.1935 ± 0.0953	0.0185 ± 0.0148	0.1046 ± 0.0509	0.1046 ± 0.0509	0.6441 ± 0.2920	0.1052 ± 0.0556
Gemma-3n-e2b-it	0.0717 ± 0.0710	0.0089 ± 0.0090	0.2203 ± 0.0581	0.0331 ± 0.0175	0.1341 ± 0.0331	0.1346 ± 0.0332	0.7716 ± 0.0826	0.1116 ± 0.0411
Gemma-3-4b-it	0.1699 ± 0.0885	0.0189 ± 0.0122	0.2557 ± 0.0484	0.0382 ± 0.0203	0.1341 ± 0.0271	0.1341 ± 0.0271	0.7875 ± 0.0203	0.1514 ± 0.0412
Gemma-3n-e4b-it	0.0058 ± 0.0304	0.0007 ± 0.0037	0.0127 ± 0.0509	0.0021 ± 0.0094	0.0072 ± 0.0288	0.0072 ± 0.0288	0.0471 ± 0.1844	0.0067 ± 0.0281
Medgemma-4b-it	0.0559 ± 0.0660	0.0069 ± 0.0080	0.1591 ± 0.0959	0.0208 ± 0.0191	0.0917 ± 0.0535	0.0917 ± 0.0535	0.6073 ± 0.3121	0.0820 ± 0.0520
Llama-3.2-1b-instruct	0.0265 ± 0.0627	0.0033 ± 0.0074	0.1041 ± 0.0723	0.0109 ± 0.0116	0.0632 ± 0.0361	0.0632 ± 0.0361	0.6324 ± 0.2729	0.0530 ± 0.0396
Llama-3.2-3b-instruct	0.1261 ± 0.1028	0.0125 ± 0.0094	0.1995 ± 0.0806	0.0304 ± 0.0188	0.1114 ± 0.0425	0.1141 ± 0.0453	0.7328 ± 0.1553	0.1214 ± 0.0617
Llama-3.1-8b-instruct	0.1556 ± 0.0817	0.0160 ± 0.0088	0.2090 ± 0.0737	0.0305 ± 0.0170	0.1142 ± 0.0416	0.1149 ± 0.0417	0.7010 ± 0.1985	0.1298 ± 0.0506
Qwen3-1.7b	0.1772 ± 0.0999	0.0164 ± 0.0104	0.1819 ± 0.0938	0.0187 ± 0.0149	0.0982 ± 0.0498	0.0991 ± 0.0502	0.6265 ± 0.3013	0.1304 ± 0.0688
Qwen3-4b-instruct-2507	0.2260 ± 0.0592	0.0183 ± 0.0071	0.2315 ± 0.0501	0.0241 ± 0.0139	0.1162 ± 0.0254	0.1162 ± 0.0254	0.7418 ± 0.1337	0.1790 ± 0.0420
CELM-SCC	0.2991 ± 0.1276	0.0912 ± 0.0590	0.3793 ± 0.0892	0.1378 ± 0.0666	0.2441 ± 0.0771	0.2441 ± 0.0771	0.8192 ± 0.0299	0.2574 ± 0.0891
CELM	0.4652 ± 0.1884	0.2666 ± 0.1354	0.5248 ± 0.1869	0.3271 ± 0.1494	0.4339 ± 0.1767	0.4339 ± 0.1767	0.7990 ± 0.2432	0.4390 ± 0.1869

D.3. Additional Results on Alignment Module Ablation

Comprehensive results of the alignment-module ablation study on the S0002 dataset, covering settings with clinical context, without clinical context, and all cases, are summarized in Table 10. Across most evaluation settings, the SCT projector achieves significantly stronger performance than other alignment variants, highlighting the importance of modeling dependencies among EEG epoch tokens before projecting them into the LLM embedding space.

Table 10. Alignment module ablation on S0002 dataset. The best results are highlighted in orange

Projector	BLEU-1	BLEU-4	ROUGE-1	ROUGE-2	ROUGE-L	ROUGE-LSUM	BERTScore	METEOR
EEG Only								
Linear Projector	0.2644 \pm 0.0471	0.0247 \pm 0.0063	0.2928 \pm 0.0314	0.0447 \pm 0.0141	0.1392 \pm 0.0161	0.1392 \pm 0.0161	0.7828 \pm 0.0152	0.2072 \pm 0.0382
Perceiver Projector	0.2636 \pm 0.0696	0.0249 \pm 0.0098	0.2897 \pm 0.0344	0.0404 \pm 0.0146	0.1377 \pm 0.0165	0.1377 \pm 0.0165	0.7888 \pm 0.0162	0.1968 \pm 0.0385
SCT Perceiver Projector	0.2991 \pm 0.1276	0.0912 \pm 0.0590	0.3793 \pm 0.0892	0.1378 \pm 0.0666	0.2441 \pm 0.0771	0.2441 \pm 0.0771	0.8192 \pm 0.0299	0.2574 \pm 0.0891
SCT Projector	0.4652 \pm 0.1884	0.2666 \pm 0.1354	0.5248 \pm 0.1869	0.3271 \pm 0.1494	0.4339 \pm 0.1767	0.4339 \pm 0.1767	0.7990 \pm 0.2432	0.4390 \pm 0.1869
With Patient History								
Linear Projector	0.2775 \pm 0.0485	0.0283 \pm 0.0121	0.2998 \pm 0.0425	0.0507 \pm 0.0240	0.1429 \pm 0.0239	0.1473 \pm 0.0306	0.7852 \pm 0.0153	0.2143 \pm 0.0349
Perceiver Projector	0.2672 \pm 0.0556	0.0273 \pm 0.0192	0.2879 \pm 0.0378	0.0461 \pm 0.0300	0.1384 \pm 0.0281	0.1422 \pm 0.0321	0.7878 \pm 0.0159	0.1955 \pm 0.0393
SCT Perceiver Projector	0.3767 \pm 0.1557	0.1671 \pm 0.1054	0.4487 \pm 0.1283	0.2149 \pm 0.1109	0.3232 \pm 0.1263	0.3268 \pm 0.1258	0.8229 \pm 0.1341	0.3232 \pm 0.1261
SCT Projector	0.5695 \pm 0.1702	0.4145 \pm 0.1639	0.6408 \pm 0.1494	0.4805 \pm 0.1603	0.5757 \pm 0.1624	0.5772 \pm 0.1613	0.8755 \pm 0.1521	0.5597 \pm 0.1728
All								
Linear Projector	0.2762 \pm 0.0485	0.0279 \pm 0.0117	0.2991 \pm 0.0416	0.0501 \pm 0.0233	0.1426 \pm 0.0232	0.1465 \pm 0.0296	0.7849 \pm 0.0153	0.2135 \pm 0.0353
Perceiver Projector	0.2669 \pm 0.0571	0.0271 \pm 0.0184	0.2881 \pm 0.0375	0.0455 \pm 0.0288	0.1384 \pm 0.0271	0.1417 \pm 0.0309	0.7879 \pm 0.0160	0.1956 \pm 0.0392
SCT Perceiver Projector	0.3689 \pm 0.1548	0.1594 \pm 0.1042	0.4417 \pm 0.1267	0.2071 \pm 0.1098	0.3152 \pm 0.1246	0.3185 \pm 0.1243	0.8226 \pm 0.1275	0.3166 \pm 0.1245
SCT Projector	0.5590 \pm 0.1749	0.3996 \pm 0.1673	0.6292 \pm 0.1574	0.4650 \pm 0.1657	0.5614 \pm 0.1692	0.5628 \pm 0.1685	0.8678 \pm 0.1650	0.5475 \pm 0.1779

D.4. EEG Encoder Ablation

We conducted an ablation study to analyze report generation performance across different EEG encoders. Specifically, we compared CBraMod (Wang et al., 2024b) and LaBraM (Jiang et al., 2024), both EEG foundation models pretrained on large-scale EEG datasets. The results show that CBraMod consistently outperforms LaBraM, highlighting the critical role of high-quality EEG representations in effective clinical report generation.

Table 11. EEG encoder ablation study

EEG Encoder	BLEU-1	BLEU-4	ROUGE-1	ROUGE-2	ROUGE-L	ROUGE-LSUM	BERTScore	METEOR
Labram	0.4654 \pm 0.2272	0.3188 \pm 0.1904	0.5355 \pm 0.2312	0.3809 \pm 0.2027	0.4673 \pm 0.2233	0.4689 \pm 0.2231	0.7781 \pm 0.2931	0.4600 \pm 0.2259
Cbramod	0.5590 \pm 0.1749	0.3996 \pm 0.1673	0.6292 \pm 0.1574	0.4650 \pm 0.1657	0.5614 \pm 0.1692	0.5628 \pm 0.1685	0.8678 \pm 0.1650	0.5475 \pm 0.1779

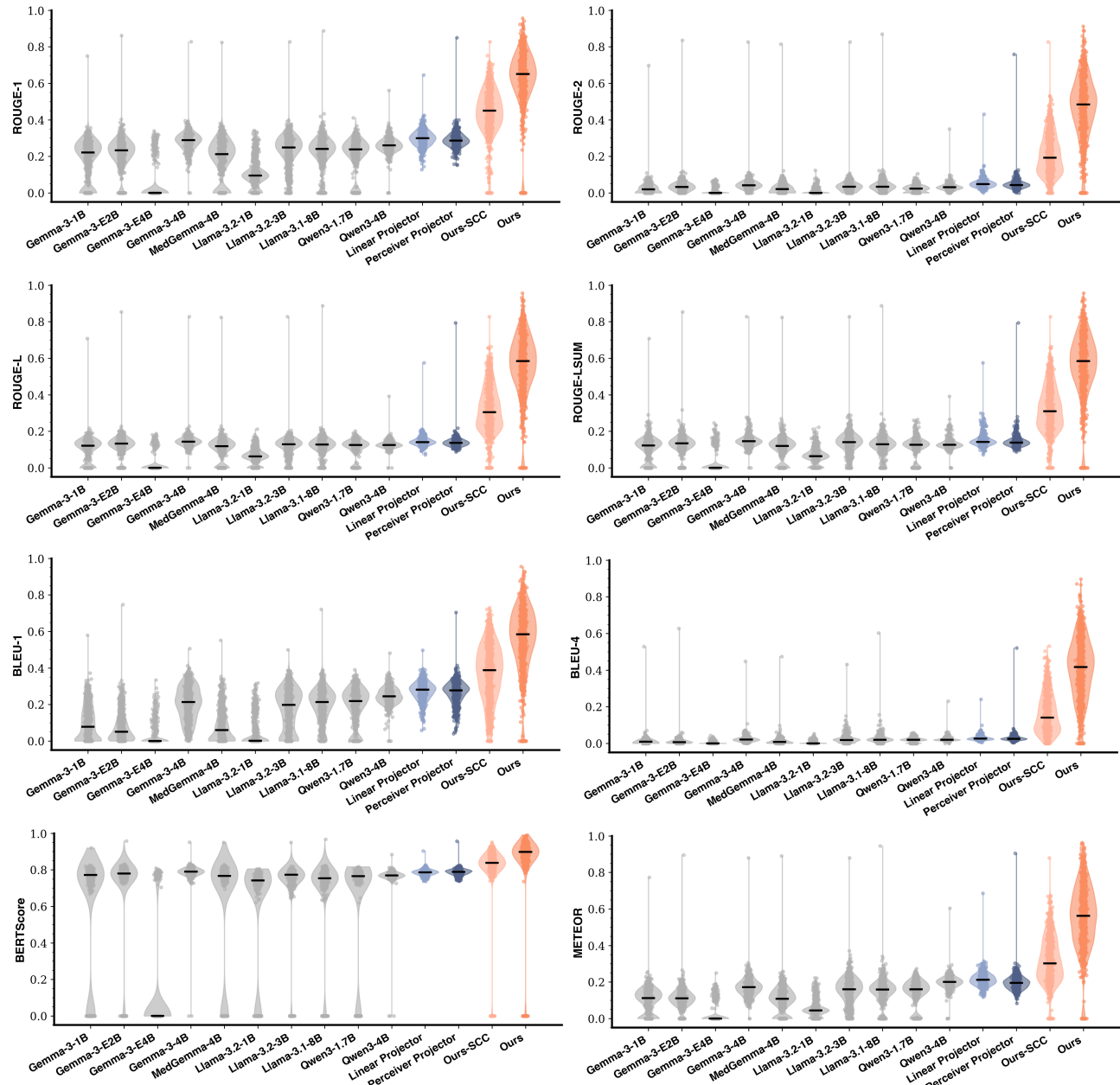
D.5. Score Distribution


Figure 9. Distribution of various metrics for overall report generation in the S0002 dataset.

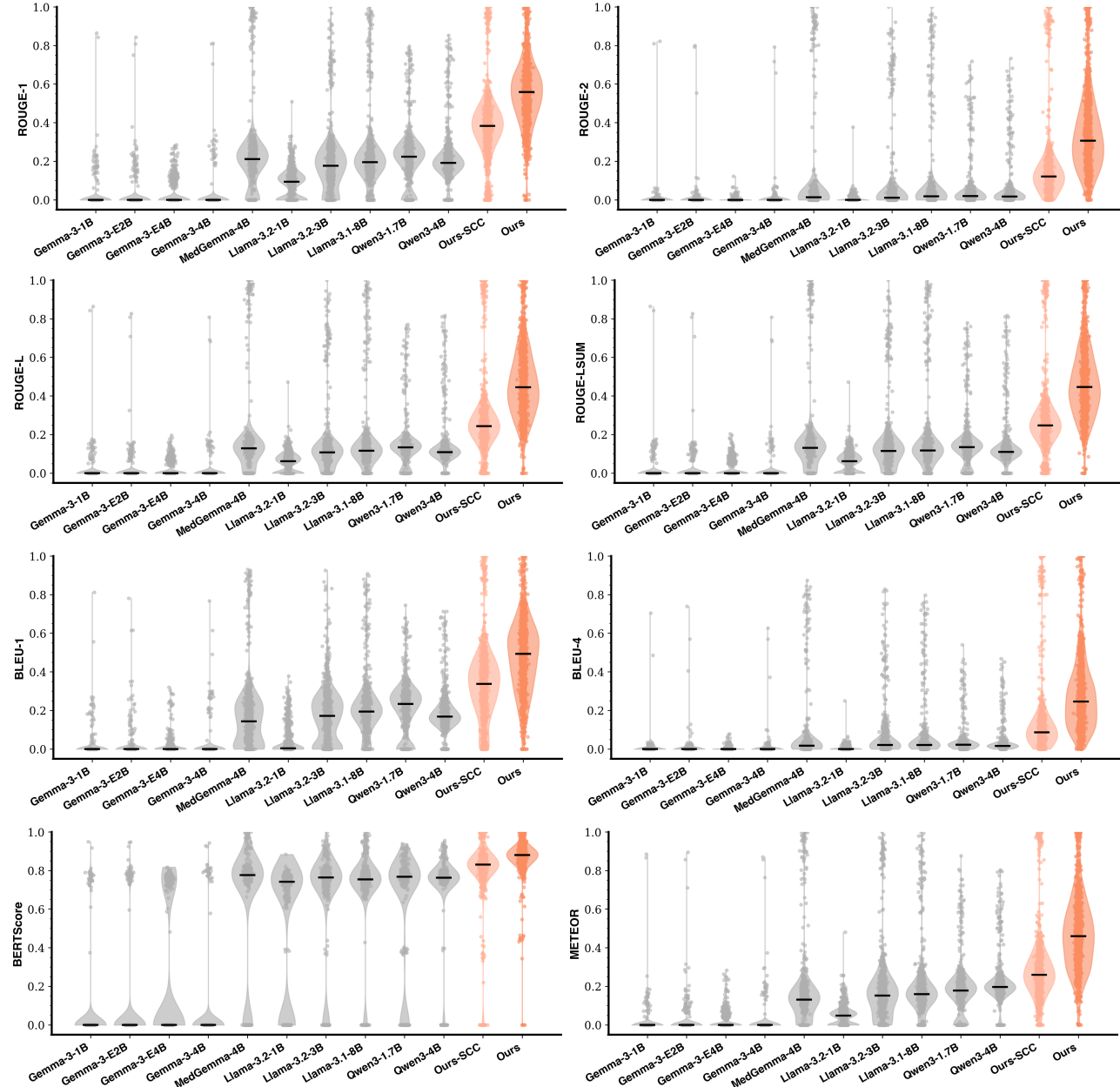


Figure 10. Distribution of various metrics for overall report generation in the S0001 dataset.

D.6. More Results on Section-wise Analysis

Table 12. Performance by report section on S0001 dataset

Report Section	Method	BLEU-1	BLEU-4	ROUGE-1	ROUGE-2	ROUGE-L	ROUGE-LSUM	METEOR
EEG Description/Details	gemma-3n-E4B-it	0.0095 ± 0.0344	0.0017 ± 0.0057	0.0396 ± 0.0604	0.0012 ± 0.0057	0.0256 ± 0.0389	0.0259 ± 0.0395	0.0228 ± 0.0385
	medgemma-4b-it	0.1624 ± 0.1729	0.0489 ± 0.1401	0.2108 ± 0.1917	0.0612 ± 0.1872	0.1460 ± 0.1858	0.1487 ± 0.1861	0.1535 ± 0.1831
	Llama-3.1-8B-Instruct	0.2045 ± 0.1452	0.0501 ± 0.1179	0.2143 ± 0.1691	0.0603 ± 0.1694	0.1454 ± 0.1687	0.1485 ± 0.1690	0.1838 ± 0.1645
	Qwen3-4B-Instruct-2507	0.1818 ± 0.0988	0.0285 ± 0.0555	0.2059 ± 0.1190	0.0393 ± 0.0969	0.1271 ± 0.1082	0.1300 ± 0.1087	0.2069 ± 0.1080
	CELM-SCC	0.3381 ± 0.1900	0.1291 ± 0.1832	0.3826 ± 0.1854	0.1601 ± 0.1935	0.2650 ± 0.1841	0.2687 ± 0.1840	0.2875 ± 0.1833
Epileptiform Abnormalities	CELM	0.4907 ± 0.1834	0.2841 ± 0.1911	0.5631 ± 0.1607	0.3483 ± 0.1987	0.4727 ± 0.1813	0.4745 ± 0.1809	0.4798 ± 0.1873
	gemma-3n-E4B-it	0.0212 ± 0.0508	0.0081 ± 0.0201	0.0256 ± 0.0642	0.0048 ± 0.0181	0.0212 ± 0.0529	0.0217 ± 0.0539	0.0193 ± 0.0563
	medgemma-4b-it	0.0015 ± 0.0117	0.0008 ± 0.0064	0.0043 ± 0.0330	0.0034 ± 0.0265	0.0043 ± 0.0330	0.0043 ± 0.0330	0.0030 ± 0.0234
	Llama-3.1-8B-Instruct	0.0786 ± 0.1185	0.0343 ± 0.0596	0.0954 ± 0.1437	0.0422 ± 0.0860	0.0858 ± 0.1337	0.0863 ± 0.1347	0.0992 ± 0.1523
	Qwen3-4B-Instruct-2507	0.0574 ± 0.0919	0.0150 ± 0.0240	0.0772 ± 0.1201	0.0273 ± 0.0473	0.0568 ± 0.0808	0.0578 ± 0.0830	0.0759 ± 0.0942
Background Activity	CELM-SCC	0.2870 ± 0.3051	0.1862 ± 0.2173	0.3392 ± 0.2614	0.2104 ± 0.2319	0.3233 ± 0.2597	0.3221 ± 0.2598	0.2717 ± 0.2560
	CELM	0.3172 ± 0.3472	0.2061 ± 0.2641	0.3881 ± 0.2967	0.2401 ± 0.2796	0.3600 ± 0.2902	0.3607 ± 0.2897	0.3222 ± 0.3107
	gemma-3n-E4B-it	0.0440 ± 0.0909	0.0058 ± 0.0113	0.0954 ± 0.1133	0.0071 ± 0.0175	0.0584 ± 0.0679	0.0584 ± 0.0679	0.0534 ± 0.0685
	medgemma-4b-it	0.0000 ± 0.0000	0.0000 ± 0.0000	0.0000 ± 0.0000	0.0000 ± 0.0000	0.0000 ± 0.0000	0.0000 ± 0.0000	0.0000 ± 0.0000
	Llama-3.1-8B-Instruct	0.0318 ± 0.0706	0.0047 ± 0.0102	0.1093 ± 0.1004	0.0102 ± 0.0181	0.0759 ± 0.0690	0.0759 ± 0.0690	0.0443 ± 0.0433
Interictal Epileptiform Abnormalities	Qwen3-4B-Instruct-2507	0.2172 ± 0.1394	0.0302 ± 0.0202	0.1984 ± 0.1289	0.0396 ± 0.0306	0.1158 ± 0.0752	0.1158 ± 0.0752	0.1492 ± 0.0969
	CELM-SCC	0.1494 ± 0.1142	0.0266 ± 0.0281	0.2442 ± 0.0629	0.0441 ± 0.0252	0.1670 ± 0.0521	0.1670 ± 0.0521	0.1355 ± 0.0524
	CELM	0.1825 ± 0.1225	0.0332 ± 0.0244	0.2703 ± 0.0536	0.0701 ± 0.0476	0.1935 ± 0.0530	0.1935 ± 0.0530	0.1786 ± 0.0655
	gemma-3n-E4B-it	0.0207 ± 0.0414	0.0096 ± 0.0192	0.0255 ± 0.0318	0.0075 ± 0.0150	0.0255 ± 0.0318	0.0255 ± 0.0318	0.0159 ± 0.0182
	medgemma-4b-it	0.0000 ± 0.0000	0.0000 ± 0.0000	0.0000 ± 0.0000	0.0000 ± 0.0000	0.0000 ± 0.0000	0.0000 ± 0.0000	0.0000 ± 0.0000
Events/Seizures	Llama-3.1-8B-Instruct	0.0891 ± 0.0899	0.0125 ± 0.0126	0.1200 ± 0.1008	0.0228 ± 0.0221	0.0672 ± 0.0550	0.0708 ± 0.0581	0.0863 ± 0.0781
	Qwen3-4B-Instruct-2507	0.1594 ± 0.0755	0.0251 ± 0.0092	0.1856 ± 0.1088	0.0334 ± 0.0218	0.0985 ± 0.0502	0.1048 ± 0.0539	0.1253 ± 0.0472
	CELM-SCC	0.0100 ± 0.0133	0.0027 ± 0.0039	0.0739 ± 0.0444	0.0228 ± 0.0140	0.0635 ± 0.0361	0.0666 ± 0.0338	0.0457 ± 0.0217
	CELM	0.0765 ± 0.0815	0.0135 ± 0.0129	0.1166 ± 0.1240	0.0236 ± 0.0232	0.0787 ± 0.0779	0.0787 ± 0.0779	0.0650 ± 0.0559
	gemma-3n-E4B-it	0.0316 ± 0.0632	0.0086 ± 0.0172	0.0497 ± 0.0696	0.0012 ± 0.0016	0.0286 ± 0.0341	0.0291 ± 0.0341	0.0364 ± 0.0610
Seizures	medgemma-4b-it	0.0000 ± 0.0000	0.0000 ± 0.0000	0.0000 ± 0.0000	0.0000 ± 0.0000	0.0000 ± 0.0000	0.0000 ± 0.0000	0.0000 ± 0.0000
	Llama-3.1-8B-Instruct	0.0448 ± 0.0551	0.0225 ± 0.0302	0.0544 ± 0.0495	0.0124 ± 0.0211	0.0528 ± 0.0497	0.0528 ± 0.0497	0.0212 ± 0.0201
	Qwen3-4B-Instruct-2507	0.0511 ± 0.0465	0.0167 ± 0.0138	0.0955 ± 0.0374	0.0040 ± 0.0071	0.0749 ± 0.0315	0.0758 ± 0.0300	0.0677 ± 0.0648
	CELM-SCC	0.0481 ± 0.0674	0.0257 ± 0.0353	0.1617 ± 0.1375	0.0004 ± 0.0009	0.1571 ± 0.1414	0.1578 ± 0.1407	0.0290 ± 0.0309
	CELM	0.0110 ± 0.0220	0.0090 ± 0.0181	0.1606 ± 0.1248	0.0024 ± 0.0033	0.1512 ± 0.1322	0.1531 ± 0.1305	0.0288 ± 0.0119
Impression/Interpretation	gemma-3n-E4B-it	0.0168 ± 0.0352	0.0032 ± 0.0070	0.0405 ± 0.0588	0.0005 ± 0.0013	0.0256 ± 0.0343	0.0300 ± 0.0409	0.0187 ± 0.0273
	medgemma-4b-it	0.0000 ± 0.0000	0.0000 ± 0.0000	0.0000 ± 0.0000	0.0000 ± 0.0000	0.0000 ± 0.0000	0.0000 ± 0.0000	0.0000 ± 0.0000
	Llama-3.1-8B-Instruct	0.0273 ± 0.0489	0.0169 ± 0.0328	0.0294 ± 0.0432	0.0010 ± 0.0026	0.0279 ± 0.0427	0.0294 ± 0.0432	0.0286 ± 0.0542
	Qwen3-4B-Instruct-2507	0.0388 ± 0.0558	0.0121 ± 0.0180	0.0790 ± 0.1025	0.0085 ± 0.0149	0.0502 ± 0.0552	0.0544 ± 0.0606	0.0464 ± 0.0543
	CELM-SCC	0.0631 ± 0.1319	0.0551 ± 0.1180	0.0773 ± 0.1057	0.0000 ± 0.0000	0.0725 ± 0.1075	0.0735 ± 0.1072	0.0336 ± 0.0502
	CELM	0.0272 ± 0.0489	0.0253 ± 0.0471	0.1390 ± 0.2061	0.0005 ± 0.0012	0.1285 ± 0.2088	0.1329 ± 0.2081	0.0419 ± 0.0545
	gemma-3n-E4B-it	0.0172 ± 0.0725	0.0108 ± 0.0622	0.0237 ± 0.0949	0.0125 ± 0.0876	0.0207 ± 0.0923	0.0207 ± 0.0923	0.0193 ± 0.0990
	medgemma-4b-it	0.0000 ± 0.0000	0.0000 ± 0.0000	0.0000 ± 0.0000	0.0000 ± 0.0000	0.0000 ± 0.0000	0.0000 ± 0.0000	0.0000 ± 0.0000
	Llama-3.1-8B-Instruct	0.0809 ± 0.1339	0.0294 ± 0.0774	0.1148 ± 0.1863	0.0489 ± 0.1334	0.0883 ± 0.1654	0.0895 ± 0.1663	0.0876 ± 0.1499
	Qwen3-4B-Instruct-2507	0.0885 ± 0.1173	0.0201 ± 0.0328	0.1069 ± 0.1399	0.0308 ± 0.0570	0.0675 ± 0.0910	0.0693 ± 0.0945	0.0996 ± 0.1172
	CELM-SCC	0.2194 ± 0.2899	0.1465 ± 0.2993	0.2687 ± 0.2946	0.1531 ± 0.3116	0.2190 ± 0.2929	0.2215 ± 0.2929	0.2206 ± 0.2996
	CELM	0.2493 ± 0.3481	0.2103 ± 0.3515	0.3581 ± 0.3381	0.2473 ± 0.3793	0.3358 ± 0.3434	0.3372 ± 0.3428	0.2829 ± 0.3428

Table 12 reports the complete section-wise performance across all models and evaluation metrics. These results extend the main text by providing detailed comparisons for each report section and further show the consistency of CELM across diverse clinical report components.

D.7. Qualitative Analysis and Case Studies

This subsection presents qualitative analyses and representative case studies to complement the quantitative evaluation. In Figure 11, 12, 13, and 14, we compare generated reports from the unimodal baseline, CELM-SCC, and CELM against ground-truth reports across multiple EEG report sections and datasets.

Qwen3-4B (Unimodal + Text + EEG Features)	Ours - SCC	Ours	Ground Truth
a. The EEG is abnormal, primarily due to diffuse theta slowing and intermittent right hemispheric delta slowing, which is consistent with encephalopathy related to post-liver transplant status. These findings are likely secondary to hepatic dysfunction affecting brain metabolism and are responsive to lorazepam as previously observed. The absence of epileptiform activity supports the diagnosis of non-epileptic encephalopathy. The clinical context of recent liver transplant and ongoing management with levetiracetam is ...	this is an abnormal eeg in the awake and drowsy states due to diffuse theta slowing of the background, as well as intermittent delta slowing in the right cerebral hemisphere. no epileptiform abnormalities were detected. none	impression: this is an abnormal eeg in the awake and drowsy states due to diffuse theta slowing of the background, as well as intermittent delta slowing in the right cerebral hemisphere. no epileptiform abnormalities were detected. none	impression: this is an abnormal eeg in the awake and drowsy states due to - diffuse theta slowing of the background, as well as intermittent delta slowing in the right cerebral hemisphere. no epileptiform abnormalities were detected. none
b.	this is a normal eeg, in the awake, drowsy and asleep states. no epileptiform abnormalities were detected. compared to the read from prior study, the present study continues to be normal. none	this is a normal eeg, in the awake, drowsy and asleep states. no epileptiform abnormalities were detected. compared to the read from prior study, the present study continues to be normal. none	impression: this is a normal eeg, in the awake, drowsy and asleep states. no epileptiform abnormalities were detected. compared to the read from prior study, the present study continues to be normal. none
c.	the eeg is normal. the patient has a history of multiple vascular and metabolic conditions. the eeg is not consistent with a diagnosis of dementia or encephalopathy. there was no evidence of seizure activity. this is a normal finding in a patient with a complex medical history.	impression: normal eeg with no epileptiform abnormalities. no significant abnormality.	impression: normal adult eeg in the awake, drowsy and stage ii sleep states. none comparison: no prior eeg available. none
d. The EEG findings are abnormal and consistent with a generalized slowing of background activity, particularly in the delta, theta, and alpha bands. The marked increase in slow-wave activity (delta and theta) and reduced alpha power suggest a state of cortical dysfunction and impaired cortical excitability. This pattern is concerning for a possible underlying epileptogenic process, especially in the context of the patient's history of complex febrile seizures. The absence of focal epileptiform discharges does not rule ...	the eeg is normal. none of the findings are consistent with complex febrile seizures. none of the findings are consistent with a neurologic abnormality.	impression: normal resting background and sleep architecture. no epileptiform abnormalities. none	impression: normal pediatric eeg in the awake, drowsy, and asleep states. none comparison: no prior eeg available. none indication: **** year old **** month old male for evaluation of complex febrile seizures (rest of clinic note was incomplete). none

Figure 11. Impression/interpretation generation examples on S0001. Examples are ordered from (a) to (d) by decreasing ROUGE-1 score. We compare outputs from the unimodal baseline (text + EEG features), CELM-SCC, CELM, and the ground-truth reports.

Qwen3-4B (Unimodal + Text + EEG Features)	Ours - SCC	Ours	Ground Truth
a. Epileptiform discharges include frequent spikes localized to the right anterior temporal region, maximal at F8, occurring during drowsiness. Additional rare spikes were observed at C3, T4, and P3. There are no runs of spike-and-wave complexes present in this recording. Previously documented asymmetric 30-40 Hz spike-and-wave activity, maximal in the left frontal region, is absent in this session. The discharges are multifocal in distribution and are consistent with a history of focal epilepsy. The spikes are not ...	there were multiple, multifocal epileptiform discharges, including: (1) frequent, bilateral, right anterior temporal spikes, maximal at f8, lasting 100-200 ms, occurring during drowsiness and wakefulness, (2), rare, bilateral, non-convulsive spikes at c3, t4, and p3, and (3) runs of asymmetric 10-12.5 hz spike-and-wave complexes, maximal at f8, lasting up to 10 seconds, without apparent clinical significance, activated by hyperventilation, and occurring spontaneously. there were no ictal ...	epileptiform abnormalities: (1) frequent epileptiform spikes during drowsiness in the right anterior temporal region (8 maximal), (2) rare spikes at c3, t4, and p3, and (3) runs of asymmetric 10-12.5 hz spike-and-wave activity, maximal in the left frontal region, lasting up to 10 seconds, without apparent clinical significance, activated by hyperventilation but also occurring spontaneously, and (3) mild continuous diffuse irregular theta-range slowing and intermittent delta slowing during wakefulness. in comparison, ...	impression: abnormal eeg due to multifocal epileptiform discharges, including (1) frequent epileptiform spikes during drowsiness in the right anterior temporal region (8 maximal), (2) rare spikes at c3, t4, and p3, and (3) runs of asymmetric 10-12.5 hz spike-and-wave activity, maximal in the left frontal region, lasting up to 10 seconds, without apparent clinical significance, activated by hyperventilation but also occurring spontaneously, and (3) mild continuous diffuse irregular theta-range slowing and intermittent delta ...
b. Interictal epileptiform discharges are abundant and predominantly localized to the left occipito-temporal region, with spike-and-wave complexes. These spikes are frequently isolated and often occur in clusters. The left anterior temporal spikes are also very frequent and may be associated with a period of activation extending to the temporal and fronto-central areas. Hyperventilation and photic stimulation were not performed during this study, and thus no reactivity was assessed. However, the pattern of discharges suggests a ...	Epileptiform discharges occurring between seizures, including morphology, lateralization, field of distribution, and activation by procedures (hyperventilation, photic stimulation).	Interictal epileptiform discharges are characterized by frequent left occipito-temporal spikes, most prominent at c3, t4, and p3. These spikes may activate a broader field over the temporal and fronto-central regions. The discharges are consistent with the patient's diagnosis of occipital epilepsy and are not triggered by specific procedures such as hyperventilation or photic stimulation.	there are at least 5 independent populations of sharp epileptiform discharges over left hemisphere, in rough order of: c3, t4, p3, f8, f7, f3, f9, t5, left anterior temporal (max f7 > t3, 13), left frontopolar (max t4 > t7, 13), left occipital (max o1, 15), and left midtemporal (max t3/t1 > f7, 15), each population is occasional in the awake and asleep background, the ratio of prevalence is 3:2:1:1:1.
c. No confirmed seizures were identified during the monitoring period. The EEG did not capture any electrographic or clinical seizures that would meet the criteria for seizure onset. The absence of ictal activity is notable given the patient's history of occipital epilepsy, but may reflect a period of relative stability. The prior report described three typical electroclinical seizures arising from the left occipital area, which were not replicated in this study. This finding should be interpreted in the ...	Specific documentation of confirmed seizure activity, including electrographic and/or clinical seizures, with details on onset time, duration, semiology, ictal EEG patterns, and post-ictal changes.	Three confirmed seizures occurred during the 5-day monitoring period. Each seizure originated from the left occipital region and was characterized by a distinct ictal EEG pattern. The onset time, duration, and semiology of each seizure were consistent with the clinical presentation of occipital epilepsy. Post-ictal changes were observed following each seizure, indicating a clear electrographic correlation with clinical events.	events/seizures: push button events. there are no ... events during the recording. seizures 1) ... 07:10:10 - 07:12:18 clinical, the patient is sleeping at the beginning of the event, and continues to sleep on his stomach for the first 50 seconds of electrographic seizure. thereafter, at 07:11:02, patient visibly arouses from sleep, and he is ... his back and extending his neck. by 07:11:29, patient is now facing the camera and his eyes can be seen to be ..., probably towards patient's ...
d.	background activity: symmetric, organized, rhythmic posterior dominant alpha frequency activity of 10-12 hz was present in the awake state. the background was symmetric, continuous and reactive to eye and/or hand movement. the patient was awake and alert throughout the recording.	the awake background was symmetric, and consisted of a 30-50uv, 8-10hz, posterior dominant rhythm which was reactive to eye opening and drowsiness, drowsiness was characterized by relative paucity of eye blink artifact, relative attenuation of the pd, relative decrease in muscle /motion artifact, and relative decrease in eye blink artifact. stage ii sleep was seen and characterized by vertex waves, k-complexes and spindles. there were no epileptiform discharges, photic stimulation was performed and produced a ...	the background is continuous, 2-6hz symmetric mixed frequency with overriding faster frequencies with no appreciable pdr or organization, there are excess left fronto-central * in isolation, maximal at f3/c3 and measuring up to 80uv, rarely these are seen on the right at t4, these do not evolve into runs. periods of active sleep are characterized by diminished myogenic artifact none photic stimulation was not performed. hyperventilation was not performed. none none ekg: regular rhythm ~ * none *, md, phd *, epilepsy ...

Figure 12. Section-wise generation examples on S0001. (a) Epileptiform abnormalities, (b) Interictal epileptiform abnormalities, (c) Seizures, and (d) Background activity. We compare outputs from the unimodal baseline (text + EEG features), CELM-SCC, CELM, and the ground-truth reports.

Qwen3-4B (Unimodal + Text + EEG Features)	Ours - SCC	Ours	Ground Truth
a. The resting background activity was asymmetric, well organized, and characterized by delta (0.5-4Hz) band power ranging from -30.50 to -21.00 dB, with a posterior dominant rhythm of 10-12 Hz over the right hemisphere and continuous 4-7 Hz activity over the left hemisphere, maximal in F3 and T3. Theta (4-8Hz) band power ranged from -33.70 to -26.20 dB, showing increased activity in the left hemisphere. Alpha (8-12Hz) band power varied from -35.80 to -24.30 dB, with a posterior dominant rhythm on the right and ...	the resting background was asymmetric, well organized, and consisted of 10-12 hz activity with up to a 12 hz posterior dominant rhythm over the right hemisphere with continuous 4-7 hz activity over the left hemisphere, maximal in f3 and t3, there were also overriding fast frequencies and 4-7 waveforms consistent with known skull ****, drowsiness was characterized by generalized slowing of the background, vertex waves, and reduced blink artifact. stage ii sleep was not seen. photic stimulation was performed ...	the resting background was asymmetric, well organized, and consisted of 10-12 hz activity with up to a 12 hz posterior dominant rhythm over the right hemisphere with continuous 4-7 hz activity over the left hemisphere, maximal in f3 and t3, there were also overriding fast frequencies and 4-7 waveforms consistent with known skull ****, none drowsiness was characterized by generalized slowing of the background, vertex waves, and reduced blink artifact. stage ii sleep was not seen. none photic stimulation ...	the resting background was asymmetric, well organized, and consisted of 10-12 hz activity with up to a 12 hz posterior dominant rhythm over the right hemisphere with continuous 4-7 hz activity over the left hemisphere, maximal in f3 and t3, there were also overriding fast frequencies and 4-7 waveforms consistent with known skull ****, none drowsiness was characterized by generalized slowing of the background, vertex waves, and reduced blink artifact. stage ii sleep was not seen. none photic stimulation ...
b. The EEG shows a background of low amplitude, slow wave activity across all frequency bands, with prominent delta (0.5-4Hz) activity, particularly in the left frontal and central regions, particularly in the left hemisphere. Theta (4-8Hz) activity is elevated, especially in the posterior regions, suggesting a state of cognitive impairment or reduced arousal. Alpha (8-12Hz) activity is reduced in amplitude, particularly in the frontal and central areas, which may reflect decreased cortical activation or attentional deficits. Beta (12-30Hz) ...	the resting background was symmetric, 10-12 hz, brisk, and showed a 10-15 uv 100% attenuation of the right anterior temporal region and a left posterior temporal region. drowsiness was characterized by a reduction in the amplitude of the background activity and the appearance of a k-complex like pattern. photic stimulation was performed and produced a robust, symmetric, and well-coupled, 10-15 hz, 150% attenuation of the anterior and posterior temporal regions. hyperventilation produced a reduction in the amplitude ...	the resting background was symmetric, and showed a well organized 8 hz, 20 uv posterior dominant rhythm which attenuated with eye opening, drowsiness was characterized by a relative paucity of eye-blink artifact and attenuation of the background rhythm. vertex waves, sleep spindles and k-complexes were seen. there were no epileptiform discharges, and there were no organized or evolving patterns suggestive of seizures. hyperventilation was not performed. photic stimulation was not performed. ekg: no dysrhythmia was ...	the resting background was symmetric, and showed a well organized 10 hz, 30-40 uv posterior dominant rhythm which attenuated with eye opening, drowsiness was characterized by a relative paucity of eye-blink artifact and attenuation of the background rhythm. stage **** sleep was not seen, no focal, lateralized or epileptiform abnormalities were seen, there were no organized or evolving patterns suggestive of seizures. photic stimulation was performed and did not produce a robust driving response. hyperventilation was not ...
c. Background activity across all channels shows a predominant slow-wave pattern with prominent delta (0.5-4Hz) activity, particularly in the left hemisphere (C3, C4, O1, O2), with values ranging from -25.20 to -120.00 dB. Theta (4-8Hz) activity is also elevated, especially in the posterior regions (P3, P4, P2), with values ranging from -24.80 to -120.00 dB. Alpha (8-12Hz) activity is present but reduced, with values ranging from -24.60 to -120.00 dB, indicating a lack of normal alpha rhythm. Beta (12-30Hz) is mildly ...	the resting background was characterized by a symmetric, well-coupled, 8-12 hz, 20-30 uv posterior dominant rhythm with 10-15 uv 50% attenuation of the anterior posterior asymmetry, there was a normal sleep architecture, including a well organized, 15-20 uv sleep spindles and 10-15 uv k-complexes. the eye blink was a normal, 10-15 uv, 10 hz, symmetric, and organized pattern. there was a normal, 10 hz, organized, 10-15 uv theta rhythm in the right anterior temporal region. photic stimulation was performed and showed a normal ...	the resting background was symmetric, and showed a well organized anterior-posterior gradient with a 9 hz, 30 uv posterior dominant rhythm which attenuated with eye opening, drowsiness was characterized by a relative paucity of eye-blink artifact, attenuation of the background rhythm and vertex waves. stage ii sleep architecture was seen and characterized by vertex waves and k-complexes, there were no epileptiform discharges, and there were no organized or evolving patterns suggestive of seizures. photic stimulation was not performed. ...	awake, at best, the background showed a 8-9 hz, 30-40 uv posterior dominant rhythm and good amplitude and organization, there was an intermittent admixed 6-7 hz 40 uv diffuse irregular theta slowing during awake state (within 1-3 seconds of eye blinking), there was near-continuous irregular ~6 hz 40 uv theta slowing over the left hemisphere, maximal over the frontal-central area, there was a continuous diffuse excess beta activity that can be seen with medication use (e.g. benzodiazepine), there ...
d. The EEG shows a background activity characterized by low amplitude, slow wave activity across all frequency bands, with prominent delta (0.5-4Hz) and theta (4-8Hz) power, particularly in the frontal and central regions. Delta power is elevated, particularly in the central channels, with values ranging from -18.60 to -25.00 dB, indicating a generalized slowing of brain activity. Theta activity is also elevated, with values ranging from -27.90 to -31.00 dB, suggesting a persistent state of slow-wave dominance. Alpha activity (8-12Hz) is ...	the background showed a well organized, symmetric, and rhythmic 3-5 hz, 15-20 microvolts, right dominant 10-15 uv, posteriorly predominated, mixed alpha activity, there was no evidence of photic stimulation, there was no evidence of a photic response: none, hyperventilation: none, sleep: none, hyperventilation: none, eye movement: none, photic: none, uv: none, photic: none, hyperventilation: none, sleep: none, hyperventilation: none, eye movement: none, ...	background activity: generalized 12-14 cycle 3-4 u.v. alpha activity, posterior dominant rhythm, no focal slowing or epileptiform discharges. sleep: no marked abnormalities. physiologic variants: none. abnormalities: none.	the resting awake background showed good bilateral symmetry, a normal anterior-posterior gradient, and a well-modulated 10 hz, 15-25 uv posterior dominant rhythm that with eye opening and closure, drowsiness and hyperventilation produced a robust, symmetric, and well-coupled, 10-15 hz, 150% attenuation of the anterior and posterior temporal regions. the eye blink and the appearance of paroxysmal theta slowing, a very brief sleep period showed poorly formed sleep spindles, photic stimulation did not produce a driving response, **** was not performed, there was continuous higher amplitude over the right frontal ...

Figure 13. EEG description/details generation examples on S0001. Examples are ordered from (a) to (d) by decreasing ROUGE-1 score. We compare outputs from the unimodal baseline (text + EEG features), CELM-SCC, CELM, and the ground-truth reports.

	Qwen3-4B (Unimodal + Text + EEG Features)	Linear Projector	Ours	Ground Truth
a.	<p>The EEG shows generalized background activity with predominant slow wave activity in the delta (0.5-4Hz) and theta (4-8Hz) bands, indicating a state of reduced cortical arousal and possible cognitive slowing. Delta power is elevated in multiple channels, particularly in the posterior regions (e.g. O1, O2, P3, P4), with values ranging from -20.00 to -24.00 dB, suggesting increased slow wave activity consistent with age-related changes and chronic medical conditions. Theta activity is also markedly elevated, with values ranging from -42.60 to -46.00 dB, particularly in the frontal and parietal regions, reflecting a state of...</p>	<p>The EEG background activity is characterized by a slow, diffusely abnormal rhythm with prominent theta and alpha activity, particularly in the posterior regions (C3, C4, O1, O2, Cz). There is a marked reduction in alpha wave amplitude, with intermittent bursts of slow-wave activity, suggesting underlying cortical dysfunction. The posterior channels (O1, O2, P3, P4, F8, Fz, Fp1, Fp2, Fp2) demonstrate minimal rhythmic activity, consistent with possible frontal lobe involvement or reduced cortical engagement. Occipital and parietal channels (P3, P4, Pz, T3, T4, T5, T6, A1, A2) show sparse activity, with no clear evidence of seizure-...</p>	<p>the waking background shows fair organization, consisting of predominantly 20-30 v, 10 hz symmetric posterior alpha activity, reactive to eye opening, there is moderate beta activity bilaterally, there is moderate theta activity bilaterally, intermittent drowsiness is characterized by attenuation of the background, slow roving eye movements and bilateral slowing in the theta and delta range with shifting predominance, stage n2 sleep is not achieved, hyperventilation is not performed, photic stimulation results in mild driving bilaterally, single lead ekg shows an apparent sinus rhythm of approximately 70 ...</p>	<p>the waking background shows good organization, consisting of predominantly 20-40 v, 10 hz symmetric posterior alpha activity, reactive to eye opening, there is moderate beta activity bilaterally, intermittent drowsiness is characterized by attenuation of the background, slow roving eye movements and bilateral slowing in the theta and delta range with shifting predominance, stage n2 sleep is not achieved, hyperventilation is not performed, photic stimulation results in moderate bilateral driving responses, single lead ekg shows an apparent sinus rhythm of approximately 60-70 beats per minute, this routine ...</p>
b.	<p>The EEG shows generalized background activity with predominantly slow wave activity in the delta (0.5-4Hz) and theta (4-8Hz) bands, indicating a low-frequency, slow-wave dominant pattern. Delta power is elevated in multiple channels, particularly in the posterior regions (e.g. O1, O2, Cz), with values ranging from -24.40 to -28.00 dB, suggesting possible cortical slowing. Theta band power is also elevated, with values ranging from -10.90 to -47.3 dB, especially in the frontal and central regions, reflecting a high degree of theta activity. Alpha band power is moderately reduced, with values ranging from -16.4 to -45.3 dB, indicating a...</p>	<p>The EEG background activity is characterized by a moderately slow, bilateral, symmetrical pattern with diffuse theta activity predominant in the 4-7 Hz range, particularly over the posterior and central regions. Alpha activity is present in the frontal and midline areas and is diminished in the parietal and occipital regions. There are no prominent spikes, sharp waves, or epileptiform discharges identified. The rhythm is relatively regular with no evidence of periodic lateralized epileptiform discharges or burst-suppression patterns. Sleep stages were not recorded, and thus no assessment of sleep architecture was...</p>	<p>the waking background shows good organization, consisting of predominantly 20-40 v, 9 hz symmetric posterior alpha activity, reactive to eye opening, there is moderate beta activity bilaterally, there is moderate theta activity bilaterally, intermittent lateral temporal slowing at 2-3 hz, intermittent driving responses are characterized by attenuation of the background, slow roving eye movements and bilateral slowing in the theta and delta range with shifting predominance, stage n2 sleep is not achieved, hyperventilation results in mild bilateral shifting, photic stimulation results in mild bilateral driving, single lead ekg shows an apparent sinus rhythm of ...</p>	<p>the waking background shows good organization, consisting of predominantly 20-40 v, 9-10 hz symmetric posterior dominant rhythm, reactive to eye opening, there is moderate beta activity bilaterally, intermittent slowing is characterized by attenuation of the background, slow roving eye movements and bilateral slowing in the theta and delta range with shifting predominance, stage n2 sleep is not achieved, hyperventilation is not performed, photic stimulation results in mild bilateral driving responses, single lead ekg shows an apparent sinus rhythm of approximately 82 beats per minute, this routine ...</p>
c.	<p>The EEG shows a background activity characterized by low to moderate amplitude, predominantly slow wave activity in the delta and theta frequency bands across multiple channels. Delta activity (0.5-4Hz) is present with values ranging from -25.80 to -29.30 dB, indicating a relatively high level of inhibition, particularly in the frontal and central regions. Theta activity (4-8Hz) is also elevated, with values ranging from -31.30 to -36.30 dB, suggesting increased theta power, especially in posterior and central regions. Alpha activity (8-12Hz) is moderately reduced, with values ranging from -29.90 to -32.70 dB, indicating a...</p>	<p>The EEG background activity is characterized by regular, bilateral, and symmetric beta and theta rhythms, with a predominant theta activity in the 4-7 Hz range, particularly over the frontal and central regions. Background alpha activity is generally smooth and rhythmic with evidence of prominent slowing or deceleration. No epileptiform discharges were identified during the recording period. The sleep stages were not fully assessed due to the patient's reported history of suspected seizures and the absence of a sleep study. Physiologic variants such as microsystoles and occasional eye movements were noted, ...</p>	<p>the waking background is mostly characterized by a good effort of 30-50 uv, 10 hz posterior dominant rhythm, with moderate reactivity, there is moderate beta activity bilaterally, there is frequent bilateral theta and alpha slowing, often with sharp temporo-occipital transients, there is a transient brief bilateral beta waves, intermittent drowsiness is characterized by attenuation of the background, slow roving eye movements and bilateral slowing in the theta and delta range with shifting predominance, stage n2 sleep is not achieved, hyperventilation is not performed, photic stimulation results in driving bilaterally, single lead ekg shows an apparent sinus rhythm of ...</p>	<p>this is a routine eeg with anterior temporal as well as standard ***** electrodes with ***** below 5 ohms, the record shows a good organization at rest, with the best waking rhythm consisting of 20-40 uv, nonstationary 6-8 hz with good reactivity, there is predominance of the fast rhythm within the right central area (probably one of the areas of **** defect), independently, there is semi-rhythmic 4 hz theta seen over the left temporal area intermittently, as well as independently on the right at different times, multiple twitches were recorded without clear change in ****, except for the myogenic ...</p>
d.	<p>The EEG shows generalized background activity with prominent delta and theta wave activity across multiple channels, particularly in the frontal and central regions. Delta power (0.5-4 Hz) is elevated in several channels with values ranging from -23.80 to -120.00 dB, indicating increased slow-wave activity. Theta band (4-8 Hz) power is also elevated, with values ranging from -23.80 to -120.00 dB, suggesting persistent slow oscillations. Alpha band (8-12 Hz) activity is moderately reduced, with values ranging from -29.90 to -120.00 dB, and beta and gamma band power shows variable reductions, particularly in the gamma range, ...</p>	<p>Background activity is best described as slow, irregular, and predominantly theta-dominant with prominent theta rhythms in the 4-7 Hz range, particularly over the occipital and parietal regions. The background shows intermittent alpha activity in the 8-13 Hz range, primarily in the frontal and central regions, with occasional suppression-burst patterns. No clear, consistent beta activity is observed. The background is generally non-regular and shows intermittent bursts of rhythmic activity, particularly in the 3-5 Hz range, which may reflect epileptiform discharges. No clear sleep stages were documented due ...</p>	<p>the waking background shows good organization, consisting of predominantly 20-40 v, 11 hz symmetric posterior alpha activity with good reactivity, there is moderate beta activity bilaterally, intermittent drowsiness is characterized by attenuation of the background, roving eye movements and bilateral slowing in the theta and delta range with shifting predominance, stage n2 sleep is not achieved, hyperventilation is not performed, photic stimulation results in mild bilateral driving responses, single lead ekg shows an apparent sinus rhythm of approximately 60-70 beats per minute, this routine ...</p>	<p>the waking background shows good organization, consisting of predominantly 30-40 v, 5-6 hz posterior background activity with fair to good reactivity and absence of background slowing, there is marked beta activity bilaterally, the record is dominated by frequent, multifocal epileptiform discharge as follow: 1) frequent to near continuous spike and wave discharges, at times periodic and in one instance progressing to an electrographic seizure from the right-left parasagittal region (4x3 and ***** with shifting maximum), 2) less frequent, independent right temporal spikes discharges (maximum t6); and 3) ...</p>

Figure 14. EEG description/details generation examples on S0002. Examples are ordered from (a) to (d) by decreasing ROUGE-1 score. We compare outputs from the unimodal baseline (text + EEG features), CELM-SCC, CELM, and the ground-truth reports.